frontiers in Pharmacology

ORIGINAL RESEARCH
published: 15 December 2021
doi: 10.3389/fphar.2021.791059

Yi-Zhi-Fang-Dai Formula Exerts Neuroprotective Effects Against Pyroptosis and Blood–Brain Barrier–Glymphatic Dysfunctions to Prevent Amyloid-Beta Acute Accumulation After Cerebral Ischemia and Reperfusion in Rats

Zhongkuan Lyu[1†], Qiyue Li[1†], Zhonghai Yu[2†], Yuanjin Chan[1], Lei Fu[3], Yaming Li[1] and Chunyan Zhang[4*]*

[1]Geriatrics Department of Chinese Medicine, Huadong Hospital Affiliated to Fudan University, Shanghai, China, [2]Department of Traditional Chinese Medicine, Shanghai Jiao Tong University Affiliated Sixth People's Hospital, Shanghai, China, [3]Shanghai Key Laboratory of Clinical Geriatric Medicine, Huadong Hospital Affiliated to Fudan University, Shanghai, China, [4]International Medical Center of Traditional Chinese Medicine, Haikou Hospital of Traditional Chinese Medicine, Haikou, China

OPEN ACCESS

Edited by:
Fang Pan,
Shandong University, China

Reviewed by:
Brad A. Sutherland,
University of Tasmania, Australia
Lumei Liu,
North Carolina Agricultural and Technical State University, United States

***Correspondence:**
Yaming Li
doctorymli@163.com
Chunyan Zhang
cyzhang0810@163.com

[†]These authors have contributed equally to this work and share first authorship

Specialty section:
This article was submitted to Ethnopharmacology, a section of the journal Frontiers in Pharmacology

Received: 07 October 2021
Accepted: 29 November 2021
Published: 15 December 2021

Citation:
Lyu Z, Li Q, Yu Z, Chan Y, Fu L, Li Y and Zhang C (2021) Yi-Zhi-Fang-Dai Formula Exerts Neuroprotective Effects Against Pyroptosis and Blood–Brain Barrier–Glymphatic Dysfunctions to Prevent Amyloid-Beta Acute Accumulation After Cerebral Ischemia and Reperfusion in Rats. Front. Pharmacol. 12:791059. doi: 10.3389/fphar.2021.791059

Background: The dysfunctional blood–brain barrier (BBB)–glymphatic system is responsible for triggering intracerebral amyloid-beta peptide (Aβ) accumulation and acts as the key link between ischemic stroke and dementia dominated by Alzheimer's disease (AD). Recently, pyroptosis in cerebral ischemia and reperfusion (I/R) injury is demonstrated as a considerable mechanism causing BBB–glymphatic dysfunctions and Aβ acute accumulation in the brain. Targeting glial pyroptosis to protect BBB–glymphatic functions after cerebral I/R could offer a new viewpoint to prevent Aβ accumulation and poststroke dementia. Yi-Zhi-Fang-Dai formula (YZFDF) is an herbal prescription used to cure dementia with multiple effects of regulating inflammatory responses and protecting the BBB against toxic Aβ-induced damage. Hence, YZFDF potentially possesses neuroprotective effects against cerebral I/R injury and the early pathology of poststroke dementia, which evokes our current study.

Objectives: The present study was designed to confirm the potential efficacy of YZFDF against cerebral I/R injury and explore the possible mechanism associated with alleviating Aβ acute accumulation.

Methods: The models of cerebral I/R injury in rats were built by the method of middle cerebral artery occlusion/reperfusion (MCAO/R). First, neurological function assessment and cerebral infarct measurement were used for confirming the efficacy of YZFDF on cerebral I/R injury, and the optimal dosage (YZFDF-H) was selected to conduct the experiments, which included Western blotting detections of pyroptosis, $A\beta_{1\text{-}42}$ oligomers, and NeuN, immunofluorescence observations of glial pyroptosis, aquaporin-4 (AQP-4), and Aβ locations, brain water content measurement, SMI 71 (a specific marker for BBB)/

AQP-4 immunohistochemistry, and Nissl staining to further evaluate BBB–glymphatic functions and neuronal damage.

Results: YZFDF obviously alleviated neurological deficits and cerebral infarct after cerebral I/R in rats. Furthermore, YZFDF could inactivate pyroptosis signaling via inhibiting caspase-1/11 activation and gasdermin D cleavage, ameliorate glial pyroptosis and neuroinflammation, protect against BBB collapse and AQP-4 depolarization, prevent Aβ acute accumulation and $A\beta_{1\text{-}42}$ oligomers formation, and reduce neuronal damage and increase neurons survival after reperfusion.

Conclusion: Our study indicated that YZFDF could exert neuroprotective effects on cerebral I/R injury and prevent Aβ acute accumulation in the brain after cerebral I/R associated with inhibiting neuroinflammation-related pyroptosis and BBB–glymphatic dysfunctions.

Keywords: Yi-Zhi-Fang-Dai formula, cerebral ischemia and reperfusion injury, dementia, neuroinflammation, pyroptosis, blood–brain barrier–glymphatic system, aquaporin-4, amyloid-beta peptide

INTRODUCTION

Alzheimer's disease (AD), a common neurodegenerative disease, comprises the major type of dementia and is causing a high socioeconomic impact with the advancement of world population aging (Alzheimer's Association, 2021). It is known that amyloid-beta peptide (Aβ) accumulation acts as a core factor among the multifaceted etiology of AD, which is closely associated with the cerebrovascular dysfunctions, especially brain microcirculation disturbance (Bell and Zlokovic, 2009; Yamazaki and Kanekiyo, 2017; Jack et al., 2018; Hampel et al., 2021; Kim et al., 2021). Experimental and clinical research is emerging to indicate that cerebral ischemia and reperfusion (I/R) can trigger both acute and chronic accumulation of Aβ in the brain which exacerbates cerebral I/R injury and accounts for the occurrence of dementia induced by ischemic stroke (van Groen et al., 2005; Song et al., 2013; Liu et al., 2015; Martins et al., 2019). Thus, maintaining the clearance of Aβ after cerebral I/R could offer a new therapeutic approach to prevent poststroke cognitive impairment and development into dementia (Goulay et al., 2020).

The normal blood–brain barrier (BBB) is an essential condition for keeping the balance of intracerebral and extracerebral Aβ, and accordingly BBB breakdown has been demonstrated as an early biomarker prior to appearance of cognitive impairment (Nation et al., 2019; Hussain et al., 2021). In addition to the BBB, the glymphatic system is another considerable pathway for the clearance of Aβ in the brain (Tarasoff-Conway et al., 2015). Endfeet of astrocytes are the main components of both the BBB and glymphatic system which contribute to maintain the homeostasis of brain microenvironments, and aquaporin-4 (AQP-4) on astrocytic endfeet is a water channel protein with high polarization and essential for neurovascular coupling and glymphatic flow to facilitate the clearance of metabolites such as Aβ (Nakada et al., 2017). Thus, in cerebral I/R injury, the loss of AQP-4 polarization on astrocytic endfeet is considered as an important factor of BBB–glymphatic dysfunctions that are the vital pathological change causing the onset and development of dementia (Verheggen et al., 2018; Goulay et al., 2020).

Inflammation is inherent across the whole course of both ischemia and reperfusion stages, and accordingly neuroinflammation acts as the fundamental cause and meanwhile as the consequence of cerebral I/R injury (Liu et al., 2014; Du et al., 2021). Recently, pyroptosis, a pro-inflammatory cell death, has been demonstrated as a crucial pathological link and gasdermin D (GSDMD) as its key effector in cerebral I/R injury (Zhang et al., 2019). Canonical pyroptosis was deemed to rely on the activation of inflammasomes represented by nucleotide-binding oligomerization domain-like receptors pyrin domain-containing 3 (NLRP3)/apoptosis-associated speck-like protein containing a caspase activation and recruitment domain (ASC)/caspase-1 to cleave GSDMD, causing the secretion of pro-inflammatory mediators such as cleaved interleukin-1β (IL-1β) (Shi J. et al., 2015). However, in the noncanonical pyroptosis pathway, GSDMD is the direct substrate of caspase-11 (orthologous caspase-4/5 in humans), and the N-terminal fragment (GSDMD-N) from the cleavage of full length GSDMD (GSDMD-FL) is critical for the formation of membrane nanopores leading to cell death. Meanwhile, as the upstream signaling, GSDMD-N activates the NLRP3/ASC/caspase-1 pathway and then results in the maturation and secretion of cleaved IL-1β (Kayagaki et al., 2015; Yi, 2018; Matikainen et al., 2020). Our recent study (Lyu et al., 2021) indicated that caspase-11-mediated pyroptosis after cerebral I/R focuses on glial cells (microglia and astrocytes) and is a considerable factor aggravating BBB–glymphatic dysfunctions and Aβ accumulation.

As one hallmark of cerebral I/R injury, BBB breakdown in the ischemic period is exacerbated by reperfusion and followed by a no-reflow phenomenon of capillaries (Mohamed Mokhtarudin and Payne, 2015; Burrows et al., 2016; Huang et al., 2020). In addition to intracerebral Aβ retention caused by microcirculation disturbance, activated platelets contained in microthrombosis during the ischemic period and after I/R are demonstrated as the potential

TABLE 1 | Components of Yi-Zhi-Fang-Dai formula.

Latin name	English name	Chinese name	Part used	Ratio (%)
Ginkgo biloba	Ginkgo biloba leaves	Yinxingye	Dry leaves	30
Panax ginseng C. A. Meyer	Ginseng	Renshen	Root and rhizome	30
Cistanche deserticola Ma	Cistanches Herba	Roucongrong	Succulent stem	30
Acorus tatarinowii	Grassleaf sweetflag rhizome	Shichangpu	Rhizome	10

peripheral source of acute Aβ accumulation in blood vessels including capillaries and nearby brain tissues (Martins et al., 2019; Carbone et al., 2021). Aβ accumulation in the brain can raise the formation of a toxic Aβ-like $Aβ_{1-42}$ oligomer, cause swelling in astrocytic endfeet, and also lead to dysregulation of capillaries by acting on pericytes, impairing energy supply for neurons (Merlini et al., 2011; Cavallucci et al., 2012; Nortley et al., 2019). Therefore, early protection of microcirculation and elimination of thromboinflammation in microcirculation after cerebral I/R are both crucial therapeutic strategies for the clearance of metabolites such as Aβ and the prevention of poststroke dementia.

According to traditional Chinese medicine (TCM) theories, blood stasis in brain collaterals with stagnancy of collateral-Qi in a deficiency condition is regarded as the basic pathogenesis of cerebral I/R injury (Wang B. et al., 2021), thus invigorating Qi and dredging brain collaterals are basic TCM therapeutic principles which consist of current therapeutic strategies emphasizing on microcirculation protection and removal of obstructions. Herbs have been widely used for thousands of years and are suitable for treating complex diseases such as ischemic stroke and dementia with the multicomponent and multitarget advantages (Yu et al., 2020; Singh et al., 2021). Yi-Zhi-Fang-Dai formula (YZFDF) is an experiential herbal prescription (Chan et al., 2020) commonly used to cure dementia cases by multiple efficacies of invigorating Qi, dredging brain collaterals, and promoting neurological function recovery. YZFDF is purely composed of herbal medicines with various bioactive ingredients, such as bilobalide, ginkgolide A, ginsenoside Rg1, cistanoside A, and α-asarone (Liu et al., 2016a). Our previous work showed that YZFDF and EGb761, the extracts from its main herb (*Ginkgo biloba* leaves), can inhibit microglial activation, regulate inflammatory responses, and protect the BBB against toxic Aβ-induced damage *in vitro* and *in vivo* (Wan WB. et al., 2014; Wan et al., 2016; Chan et al., 2020). Therefore, based on our previous studies, the present study was designed to confirm the potential therapeutic effects of YZFDF against cerebral I/R injury and further preliminarily explore the possible mechanism associated with alleviating Aβ acute accumulation by anti-neuroinflammation–related pyroptosis and BBB–glymphatic dysfunctions.

MATERIALS AND METHODS

Components and Drug Powder Preparation of YZFDF

YZFDF comprises four herbs as shown in **Table 1**, including *Ginkgo Biloba* leaves, Ginseng, Cistanches Herba, and grassleaf sweetflag rhizome, which were purchased from Shanghai Hongqiao Pharmaceutical Co., Ltd. (Shanghai, China). These herbal medicines were identified by the TCM Preparation Room of Shanghai Geriatric Institute of Chinese Medicine, Shanghai University of Traditional Chinese Medicine. The main active ingredient analysis of YZFDF by the methods of high-performance liquid chromatography (HPLC) and mass spectrometry (MS), as well as the chemical structures of each ingredient were introduced in detail in our previous work (Liu et al., 2016a). The YZFDF drug powder was prepared as previously described (Liu et al., 2016a; Chan et al., 2020). In brief, four herbal medicines were subjected twice to extraction with 75% ethanol for 2 h. The herbal dregs of the extract solution were removed after filtering. Subsequently, the filtered liquid was concentrated using a rotary evaporator (BÜCHI Labortechnik AG, Flawil, Switzerland) and then dried to get a drug powder by the freeze-drying method. The YZFDF power was kept in an airtight container in the deep freezer (−36°C) for long-term storage, and the powder was made into a suspension liquid nearing usage and then stored at 4°C.

Animals

All animal experiments in this study were approved by the Ethics Committee of Shanghai Jiao Tong University Affiliated Sixth People's Hospital and performed in accordance with the relevant guidelines and regulations. Efforts were made as well to minimize animal suffering during the whole experiments. Specific pathogen-free (SPF) male Sprague–Dawley (SD) rats, weighing 200–230 g, were purchased from the Shanghai Laboratory Animal Research Center (Shanghai, China). The rats were housed in a SPF barrier environment under standard conditions at a controlled temperature (23 ± 1°C) on a 12:12 h light–dark cycle. Experimental operations were carried out after the acclimation of animals for several days with free access to food and water.

Drug Administration and Experimental Design

The common human daily dosage of raw YZFDF herbs is 100 g/75 kg bodyweight. According to the formula (Lan et al., 2013) $d_{rat} = d_{human} \times 0.7/0.11$, the common dosage of raw YZFDF herbs in rats should be 8.48 g/kg/day, and the corresponding drug powder dosage is 2.69 g/kg/day. The drug tolerance of a rat is generally higher than that of the human, and thus we selected 2.8, 5.6, and 11.2 g/kg/day as the low, medium, and high drug powder dosages of YZFDF in the present study, respectively. Accordingly, at the first stage of this study, forty rats were randomly divided into five groups: sham group (Sham), ischemia and reperfusion group (I/

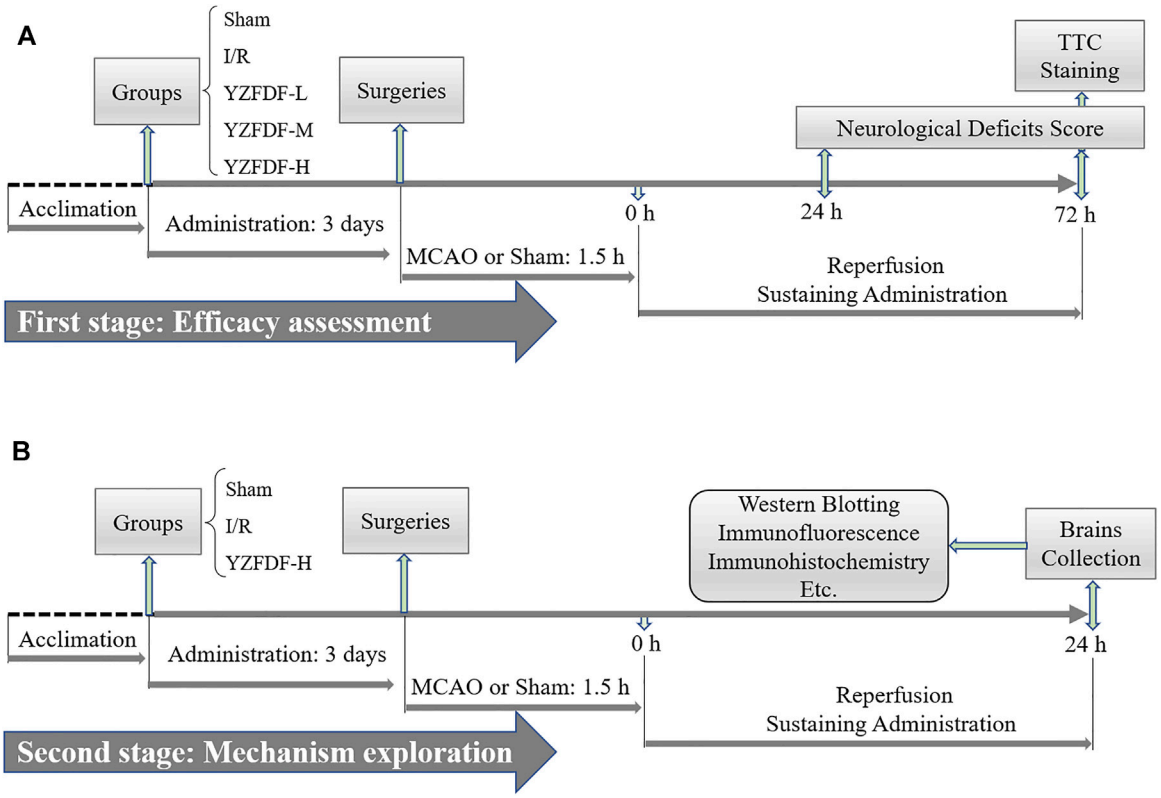

FIGURE 1 | Schematic diagram of this study. **(A)** First stage aiming at the efficacy assessment of YZFDF against I/R injury. **(B)** Second stage of this study for further preliminarily exploring the possible mechanism.

R), YZFDF low-dosage group (YZFDF-L), YZFDF medium-dosage group (YZFDF-M), and YZFDF high-dosage group (YZFDF-H). The rats in the YZFDF-treated groups were orally administered with the corresponding drug powder dosage of YZFDF (dissolved in distilled water), and the other rats were given the same volume of distilled water. Drug administration was performed twice a day at 9:00 and 16:00 for 3 days before the surgery and lasted 3 days after the surgery until animal sacrifice. According to the results of neurological function assessment and measurement of cerebral infarct area, the optimal dosage of YZFDF (YZFDF-H) was selected to conduct the following experiments.

At the second stage of this study, forty-five rats were randomly divided into three groups: sham group (Sham), ischemia and reperfusion group (I/R), and YZFDF high-dosage group (YZFDF-H). Drug administration was performed as previously mentioned for 3 days before the surgery and lasted until animal sacrifice for 24 h after reperfusion. The schematic diagram of this study is exhibited in **Figure 1**.

Focal Cerebral I/R Injury Models

The models of focal cerebral I/R injury were built by the method of left middle cerebral artery occlusion/reperfusion (MCAO/R) as described in our previous studies (Yu et al., 2016; Yu et al., 2018). In brief, rats were anesthetized with pentobarbital sodium (0.5%, 1 ml/100 g). After the skin disinfection and incision, the left common carotid artery (CCA) was identified and exposed by separation from surrounding tissues. Subsequently, the external carotid artery (ECA) and internal carotid artery (ICA) were dissected and exposed carefully. At first, the ICA was occluded using a microvascular clip and the far end of the ECA was fastened, followed by the ECA being cut at 1 cm away from the bifurcation between the ECA and ICA. Then, a nylon monofilament (Beijing Sunbio Biotech, China) was inserted into the ICA from the incision of the ECA with the microvascular clip removed. At last, resistance could be felt when the rounded tip of the monofilament reached the origin of the middle cerebral artery (MCA) at the length of 18.5–19.5 mm from the bifurcation, and then the monofilament was fastened at ECA stump. After MCAO of 1.5 h, the monofilament was withdrawn to implement reperfusion. In the present study, the rats in I/R and YZFDF-treated groups were subjected to blinded MCAO/R surgeries, while rats in the Sham group only underwent the same operation with no insertion of the monofilament. During the whole course, the cardiovascular rate and rectal temperature of all rats were monitored and maintained.

Neurological Function Assessment

Neurological examinations were performed after reperfusion. In order to exclude the interference of surgery failures, the rats subjected to MCAO/R with no detectable neurological deficits

were eliminated. The neurological deficit scores of rats at 24 and 72 h after reperfusion in the present study were evaluated on a 5-point scale as previously described (Longa et al., 1989; Cai et al., 2016): 0 = no deficit; 1 = failure to extend right forepaw; 2 = circling to the right; 3 = falling to the right; 4 = no spontaneous walking with a depressed level of consciousness.

Measurement of the Cerebral Infarct Area

The measurement of the cerebral infarct area by 2, 3, 5-triphenyl tetrazolium chloride (TTC; Nanjing Jiancheng Bioengineering Institute, Nanjing, Jiangsu, China) staining was carried out as previously described (Yu et al., 2016). In brief, at 72 h after reperfusion, the rats under deep anesthesia went through cardiac perfusion with 200 ml normal saline. Subsequently, their brains were taken out quickly and placed at −20°C for 20 min. Then, each brain was sliced into five coronal slices (2 mm thickness) from the rostral to the caudal on the frozen ice pack, and then the slices were stained with TTC solution away from light for 20 min at 37°C. As a result, the infarct brain tissue was stained to the white-colored area distinguished from the red-colored non-infarct area. After the fixation of stained brain slices with 4% paraformaldehyde for 24 h, the percentages of the cerebral infarct area were calculated by microscope image analysis software (Image-Pro Plus, United States) according to the following formula (Yu et al., 2016): [contralateral hemisphere area-(ipsilateral hemisphere area-infarct area)/2×contralateral hemisphere area] × 100%.

Brain Water Content Measurement

The dry–wet weight method was used to measure the brain water content. In Brief, the rats were sacrificed under deep anesthesia, and their brains were quickly taken out. Then, ischemic and nonischemic cerebral hemispheres were separated, immediately weighed to obtain the wet weight (WW), and then placed in an oven at 60°C for 24 h to obtain the dry weight (DW). The brain water content was calculated with the following formula (Lan et al., 2013): 100% × (WW−DW)/WW.

Western Blotting Analysis

After 24 h reperfusion, the rats were deeply anesthetized and went through cardiac perfusion. The brains were taken out, and the ischemic core and normal brain tissue were obviously visible to the naked eye. Then, the transition zone neighboring the ischemic core (ischemic penumbra) and the equivalent area under sham were quickly peeled off and stored at −80°C. Western blotting (WB) analysis was used to detect the expression levels of neuroinflammation-related pyroptosis signaling molecules, $A\beta_{1\text{-}42}$ monomer/oligomers, and NeuN (a marker of neurons). In brief, the brain tissues from ischemic penumbra and the equivalent area under sham were prepared for protein samples followed by the concentration measurement. Subsequently, corresponding protein samples with equal amounts were separated by 10% sodium dodecyl sulfate-polyacrylamide gel electrophoresis and then electrotransferred onto the poly-vinylidnene fluoride membranes. Then, the membranes were blocked by 5% bovine serum albumin (BSA) at room temperature for 1 h and incubated at 4°C overnight with the following primary antibodies (**Supplementary Table S1** for details): caspase-11 (Santa Cruz, United States), GSDMD (CST, United States), NLRP3 (ProteinTech, United States), ASC (Santa Cruz), caspase-1 (ProteinTech), IL-6 (Santa Cruz), IL-1β (Santa Cruz), ionized calcium-binding adapter molecule-1 (Iba-1) (Abcam, United Kingdom), $A\beta_{1\text{-}42}$ (Abcam), NeuN (ProteinTech), and β-actin (CST). Then, the membranes were washed and incubated with the corresponding secondary antibodies (Signalway Antibody, United States) for 1 h at room temperature. Finally, the enhanced chemiluminescence kit (Millipore, United States) was used to develop WB bands, and the intensities of bands were analyzed with ImageJ software (National Institutes of Health, United States).

Immunofluorescence

After deep anesthetization, the rats went through cardiac perfusion with 200 ml normal saline and then 4% paraformaldehyde. Subsequently, the brains were taken out and immersed in 4% paraformaldehyde for 24 h fixation and then prepared for paraffin slices. The procedure for immunofluorescence (IF) staining of proteins colocalization was as follows: after dewaxing and rehydration with gradient ethanol (100% ethanol for 5 min, 95% ethanol for 5 min, 80% ethanol for 5 min, 60% ethanol for 5 min, and H_2O for 5 min), the slices further went through antigen retrieval and permeation by 0.3% triton-X 100 followed by blockage with 5% BSA. Subsequently, the slices were incubated with the first antibodies (**Supplementary Table S1** for details) mixed with GSDMD/Iba-1, GSDMD/glial fibrillary acidic protein (GFAP), AQP-4/GFAP, and Aβ/GFAP overnight at 4°C followed by incubations with corresponding mixed secondary antibodies (Beyotime, China) for 1 h at room temperature. After DAPI staining, the laser scanning confocal microscope (Leica Wetzlar, Germany) was used for capturing fluorescent pictures in the same brain area with blinding. Three fields were randomly selected for the analysis of double-positive staining cell number or fluorescent density by ImageJ software.

Immunohistochemistry

An endothelial barrier antigen (EBA, clone: SMI 71) is a specific marker for the BBB, and AQP-4 polarization loss is an important cause of BBB–glymphatic dysfunctions responsible for Aβ accumulation. Thus, we further made evaluations of BBB–glymphatic functions by immunohistochemistry (IHC) staining of SMI 71 and AQP-4. In brief, after dewaxing and rehydration, the slices were subjected in sequence to antigen retrieval, permeation, inactivation of the endogenous catalase, and then blockage by 5% BSA. Subsequently, the slices were incubated with the anti-rat BBB antibody (SMI 71) (BioLegend, United States) and AQP-4 antibody (Santa Cruz) overnight at 4°C (**Supplementary Table S1** for details), followed by incubations with the corresponding secondary antibodies for 1 h at room temperature. Then, 3,3-diaminobenzidine tetrahydrochloride and hematoxylin were used for visualizing the slices. Finally, the light microscope was used for observing the slices and capturing the pictures in the same brain area with blinding. Three fields were randomly selected for the analysis of SMI 71 and AQP-4 staining density by ImageJ software.

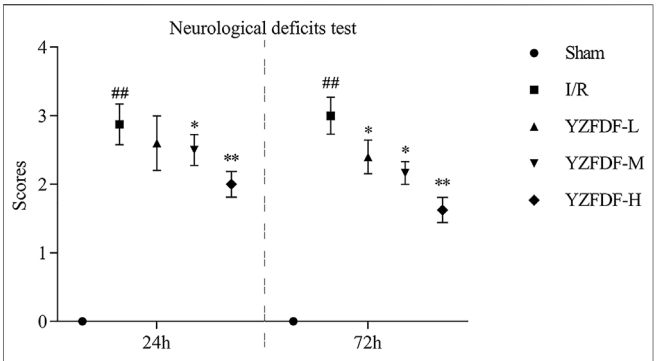

FIGURE 2 | YZFDF alleviated neurological deficits at 24 and 72 h after cerebral I/R in rats, $n = 5–8$. $^{\#\#}p < 0.01$ vs. Sham group; $^{*}p < 0.05$, $^{**}p < 0.01$ vs. I/R group.

Nissl Staining

Nissl staining was used to evaluate neuronal damage as described in our previous study (Yu et al., 2016). In brief, after dewaxing and rehydration, the slices were stained with Nissl staining solution (Sangon Biotech, China) for 20 min at room temperature. Subsequently, the slices were rinsed in graded ethanol, transparentized by xylene, and coverslipped under Permount. Finally, the pictures in the same brain area were captured with blinding using the light microscope. Four fields were randomly selected for the analysis of damaged neurons.

Statistical Analysis

All data were expressed as the mean ± standard deviation (SD) or standard error of the means (SEM). GraphPad Prism 8.0 (GraphPad Software Inc. United States) was used for statistical analysis. The differences among groups were analyzed by one-way ANOVA or unpaired Student's t-test. A value of $p < 0.05$ was considered to be statistically significant.

RESULTS

Yi-Zhi-Fang-Dai Formula Alleviated Neurological Deficits After Cerebral I/R in Rats

First, the effects of YZFDF on neurological deficits were assessed at 24 and 72 h after reperfusion in the present study. As exhibited in **Figure 2**, the rats in the Sham group had no performance of neurological deficits, and the rats in the I/R group showed obvious neurological deficits at both 24 and 72 h after reperfusion. However, compared with that of the I/R group, YZFDF-treated groups showed significantly low neurological deficit scores at 24 h (YZFDF-M group, $p < 0.05$; YZFDF-H group, $p < 0.01$) and 72 h (YZFDF-L and YZFDF-M groups, $p < 0.05$; YZFDF-H group, $p < 0.01$) after reperfusion. Thus, the result of neurological deficit assessment indicated that YZFDF could alleviate neurological deficits after cerebral I/R in a dosage- and time-dependent manner.

Yi-Zhi-Fang-Dai Formula Reduced Cerebral Infarct After Cerebral I/R in Rats

The effects of YZFDF on cerebral infarct were measured following neurological deficit assessment at 72 h after reperfusion. The result (**Figures 3A,B**) showed that the rats in the Sham group had no cerebral infarct, and the rats in the I/R group exhibited obvious cerebral infarct (white-colored area). However, compared with that of the I/R group, YZFDF-treated groups showed significantly little cerebral infarct area with the YZFDF-H group exerting optimal effects (YZFDF-L and YZFDF-M groups, $p < 0.05$; YZFDF-H group, $p < 0.01$), which was consistent with the result of neurological deficit assessment.

Based on the outcomes at the first stage of this study and our previous work, the following experiments selected the optimal dosage of YZFDF (YZFDF-H) to further explore the potential effects of YZFDF against the fundamental and crucial links in cerebral I/R injury represented by neuroinflammation-related pyroptosis, BBB–glymphatic dysfunctions, and Aβ acute accumulation and thus to preliminarily probe into its neuroprotective mechanism for preventing early pathological changes of poststroke dementia.

Yi-Zhi-Fang-Dai Formula Alleviated Cerebral I/R–Induced Pyroptosis *via* Inhibiting the Activation of Caspase-11/1 and Cleavage of GSDMD

Our previous study revealed that cerebral I/R activates the caspase-11/GSDMD-mediated pyroptosis pathway. In the present study, the result showed that YZFDF could obviously downregulate the increased protein levels of GSDMD-FL/N (the key effector of pyroptosis) and the related upstream or downstream signaling including pro/cleaved-caspase-11, NLRP3, ASC, and pro/cleaved-caspase-1 after cerebral I/R (**Figures 4A–D**), indicating that YZFDF could exert inhibitory effects on cerebral I/R–induced pyroptosis.

Yi-Zhi-Fang-Dai Formula Blocked Overactivation and Pyroptosis of Microglia and Alleviated Inflammatory Responses After Reperfusion

The inflammatory microenvironment mediated by microglial activation is inherent across the whole course of cerebral I/R injury and deteriorated by pyroptosis after reperfusion, which can be reflected by the expressions of Iba-1 (microglial biomarker), IL-6, and pyroptosis-related pro-inflammatory factors such as IL-1β. The result in the present study showed that YZFDF treatment could reduce the raised immunofluorescent co-staining of GSDMD and Iba-1 in ischemic cortex and hippocampus-CA1 areas (**Figures 5A,B**) and downregulate the expression levels of Iba-1, IL-6, and cleaved IL-1β after reperfusion (**Figures 5C,D**), indicating that YZFDF could exert inhibitory effects on inflammatory responses during cerebral I/R by regulating microglial overactivation and pyroptosis.

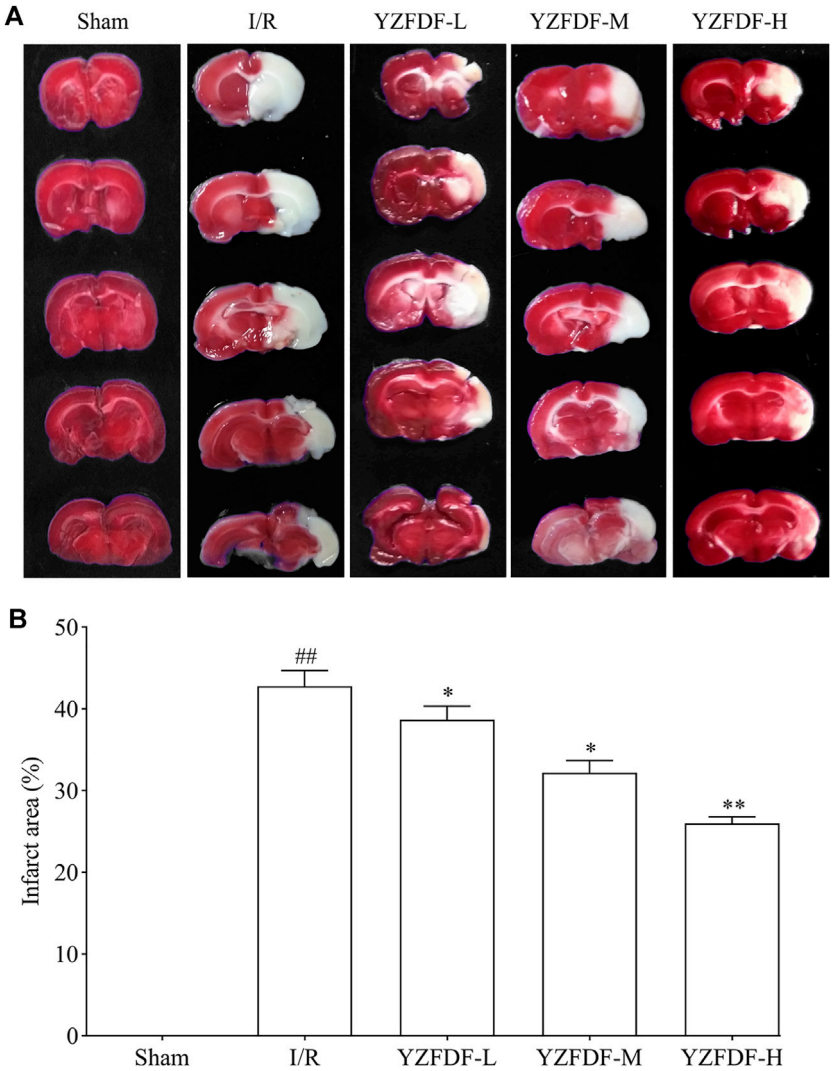

FIGURE 3 | YZFDF reduced cerebral infarct at 72 h after cerebral I/R in rats. **(A)** Representative pictures of cerebral infarct by TTC staining in each group. The red-colored area represents normal cerebral tissue with non-infarct, and the white-colored area represents cerebral infarct. **(B)** Comparative analysis of the cerebral infarct area between groups, n = 5–8. *p < 0.05, **p < 0.01 vs. I/R group.

Yi-Zhi-Fang-Dai Formula Inhibited Astrocytic Pyroptosis and Protected Against BBB Collapse After Reperfusion

Astrocytic endfeet envelop the cerebral capillaries that form the BBB. Our previous study indicated that astrocytic pyroptosis after I/R is the considerable pathological factor of BBB disruption and shriveled capillaries leading to brain microcirculation disturbance. The result in the present study showed that YZFDF treatment could reduce the GSDMD-positive immunofluorescent staining in astrocytes in ischemic cortex and hippocampus-CA1 areas (**Figures 6A,C**), indicating that YZFDF could exert inhibitory effects on cerebral I/R–induced astrocytic pyroptosis. Accordingly, YZFDF protected against BBB collapse and reduction after reperfusion which could be observed by immunohistochemical staining of SMI 71 in cortex and hippocampus-CA1 areas of the ischemic hemisphere (**Figures 6B,D,E**), potentially promoting blood flow circulation in capillaries of ischemic cerebral tissues.

Yi-Zhi-Fang-Dai Formula Restored AQP-4 Polarization and Reduced Astrocytic Endfeet Swelling and Brain Edema After Reperfusion

The loss of AQP-4 polarization on astrocytic endfeet is closely associated with BBB–glymphatic dysfunctions which promote accumulation of metabolites and brain edema. In the present study, our results exhibited the loss of AQP-4 polarization with obvious dispersion, perturbed expressions, and astrocytic endfeet swelling in the ischemic brain tissues, which could be observed by immumohistochemical staining of AQP-4 (**Figures 7A–C**) and

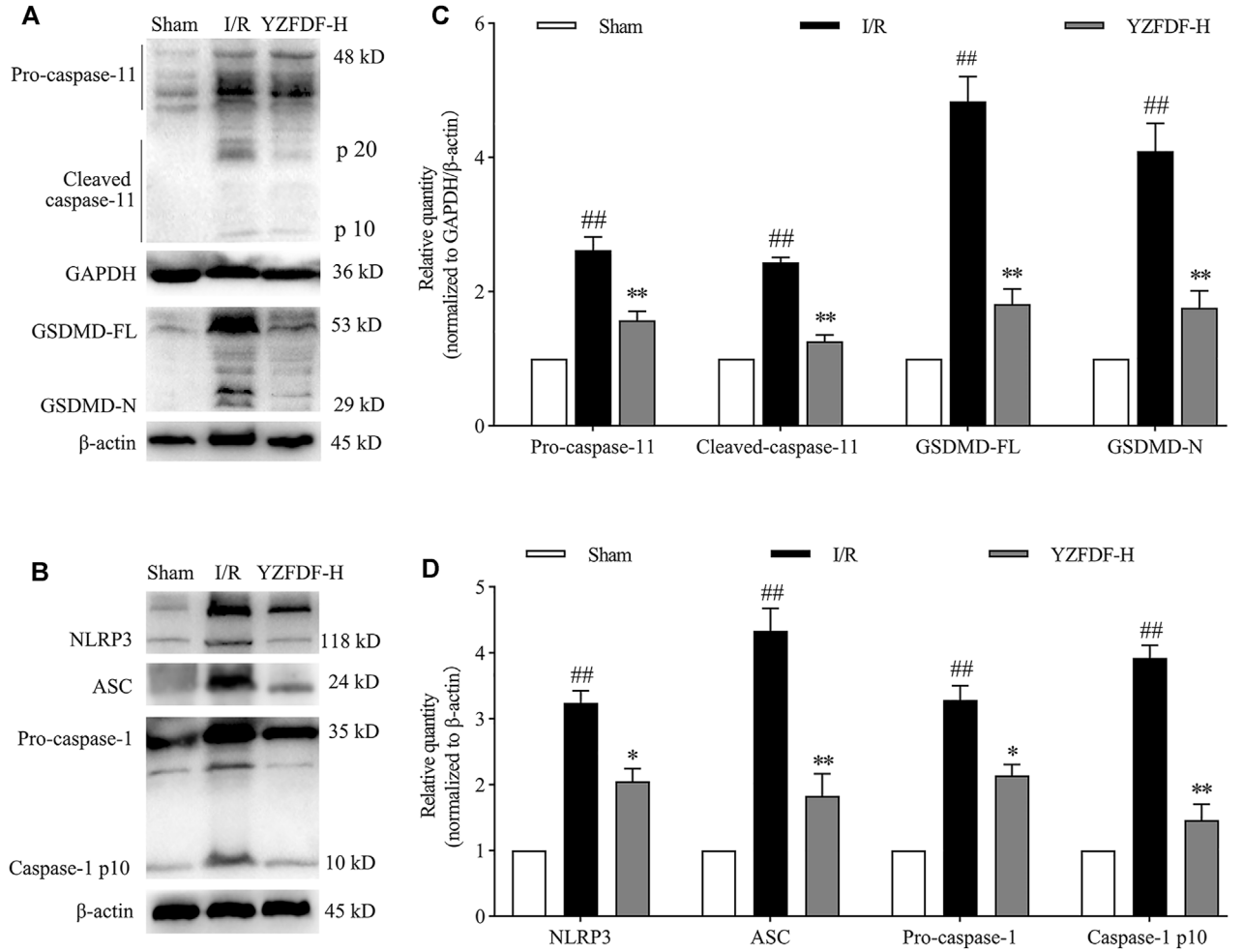

FIGURE 4 | YZFDF inhibited the activation of caspase-11/1 and cleavage of GSDMD at 24 h after cerebral I/R in rats. **(A)** Representative Western blots for pro/cleaved-caspase-11 and GSDMD-FL/N. **(B)** Representative Western blots for NLRP3, ASC, pro-caspase-1, and caspase-1 p10. **(C)** Quantitative analysis of pro/cleaved-caspase-11 and GSDMD-FL/N, $n = 6$. **(D)** Quantitative analysis of NLRP3, ASC, pro-caspase-1, and caspase-1 p10, $n = 6$. $^{\#\#}p < 0.01$ vs. Sham group; $^{*}p < 0.05$, $^{**}p < 0.01$ vs. I/R group.

double fluorescence staining of AQP-4 and GFAP in ischemic cortex and hippocampus-CA1 areas (**Figure 7D**, **Supplementary Figure S6**), while YZFDF intervention could restore AQP-4 polarization and accordingly reduce astrocytic endfeet swelling and brain edema in the ischemic hemisphere after reperfusion (**Figures 7A–E**).

Yi-Zhi-Fang-Dai Formula Promoted Aβ Clearance and Prevented the Formation of $A\beta_{1\text{-}42}$ Oligomers After Reperfusion

Based on the above results in the present study, our study further exhibited that Aβ accumulates in the sites of swelling astrocytic endfeet, which was consistent with the situation of AQP-4 polarization loss (**Figures 8A–C**). However, YZFDF treatment could alleviate Aβ acute accumulation around astrocytes within 24 h after reperfusion in ischemic cortex and hippocampus-CA1 areas (**Figures 8A–C**). Furthermore, YZFDF could prevent the formation of $A\beta_{1\text{-}42}$ oligomers (the main form of toxic Aβ) in ischemic brain tissues after reperfusion (**Figures 8D,E**).

Yi-Zhi-Fang-Dai Formula Alleviated Neuronal Damage and Promoted Neuron Survival After Reperfusion

The above results in the present study have revealed that YZFDF could inhibit cerebral I/R–induced pyroptosis, damage of the BBB–glymphatic system, and Aβ accumulation after reperfusion. Accordingly, our study further showed that YZFDF could alleviate neuronal damage after reperfusion (**Figures 9A–C**) and promote neuron survival in ischemic cortex and hippocampus-CA1 areas (**Figures 9D,E**), which was consistent with the results of the neurological function assessment and measurement of the cerebral infarct area.

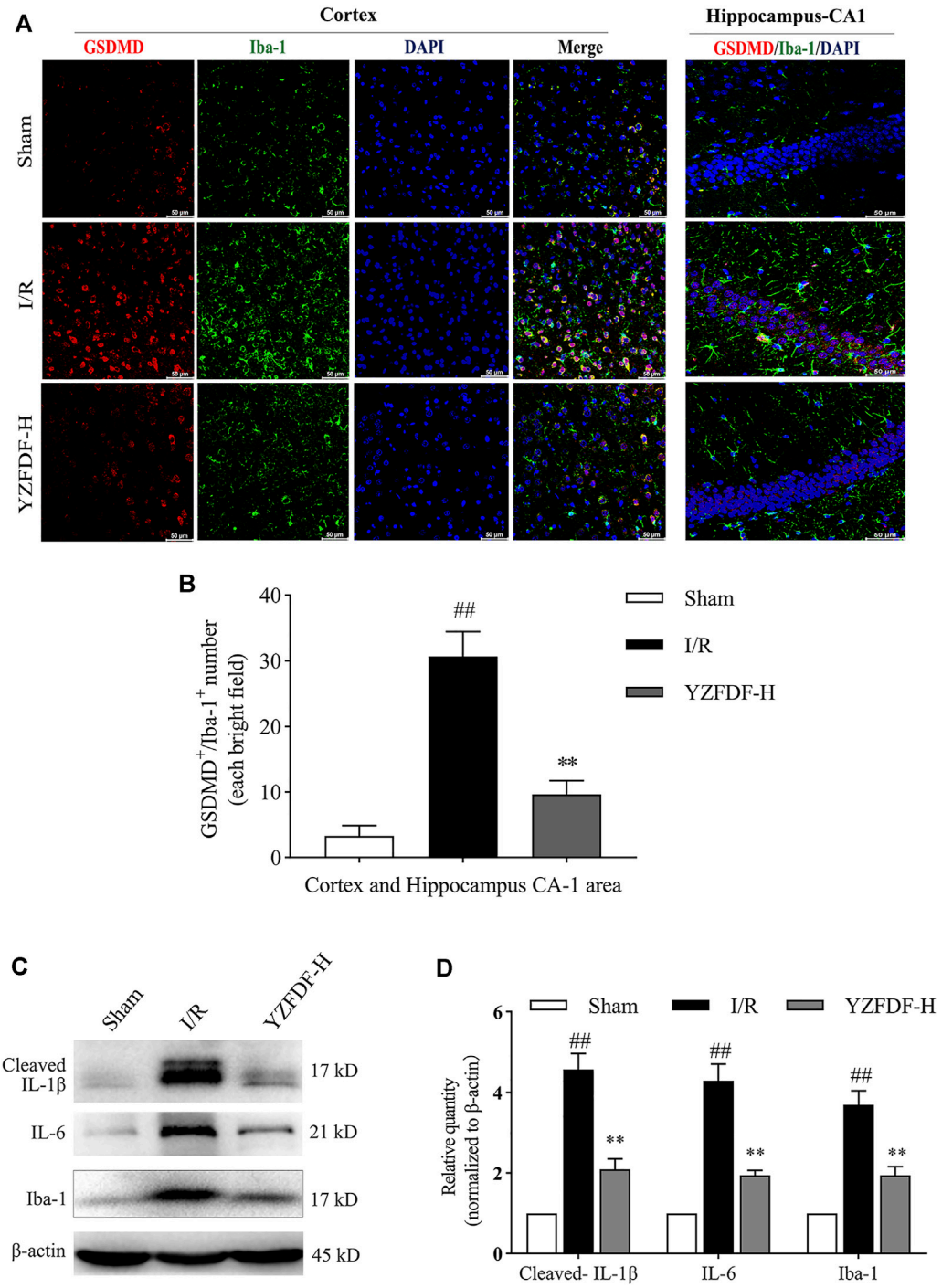

FIGURE 5 | YZFDF blocked overactivation and pyroptosis of microglia and alleviated inflammatory responses at 24 h after cerebral I/R in rats. **(A)** Representative pictures of double immunofluorescence staining of GSDMD (red) colocalized with Iba-1 (green) in cortex and hippocampus-CA1 areas, scale bar = 50 μm. **(B)** Quantitative analysis of double-positive staining of $GSDMD^{+}/Iba\text{-}1^{+}$ cell number, $n = 3$. **(C)** Representative Western blots for cleaved-IL-1β, IL-6, and Iba-1. **(D)** Quantitative analysis of cleaved-IL-1β, IL-6, and Iba-1, $n = 6$. $^{\#\#}p < 0.01$ vs. Sham group; $^{**}p < 0.01$ vs. I/R group.

DISCUSSION

AD is a chronic cerebral disease affected by multifaceted etiological factors, among which cerebrovascular diseases represented by ischemic stroke have been attracting great attention (Wang R. et al., 2021; Eskandari et al., 2021; Zupanic et al., 2021). Despite the apparent association between AD and ischemic stroke, it remains unclear how the latter induces the

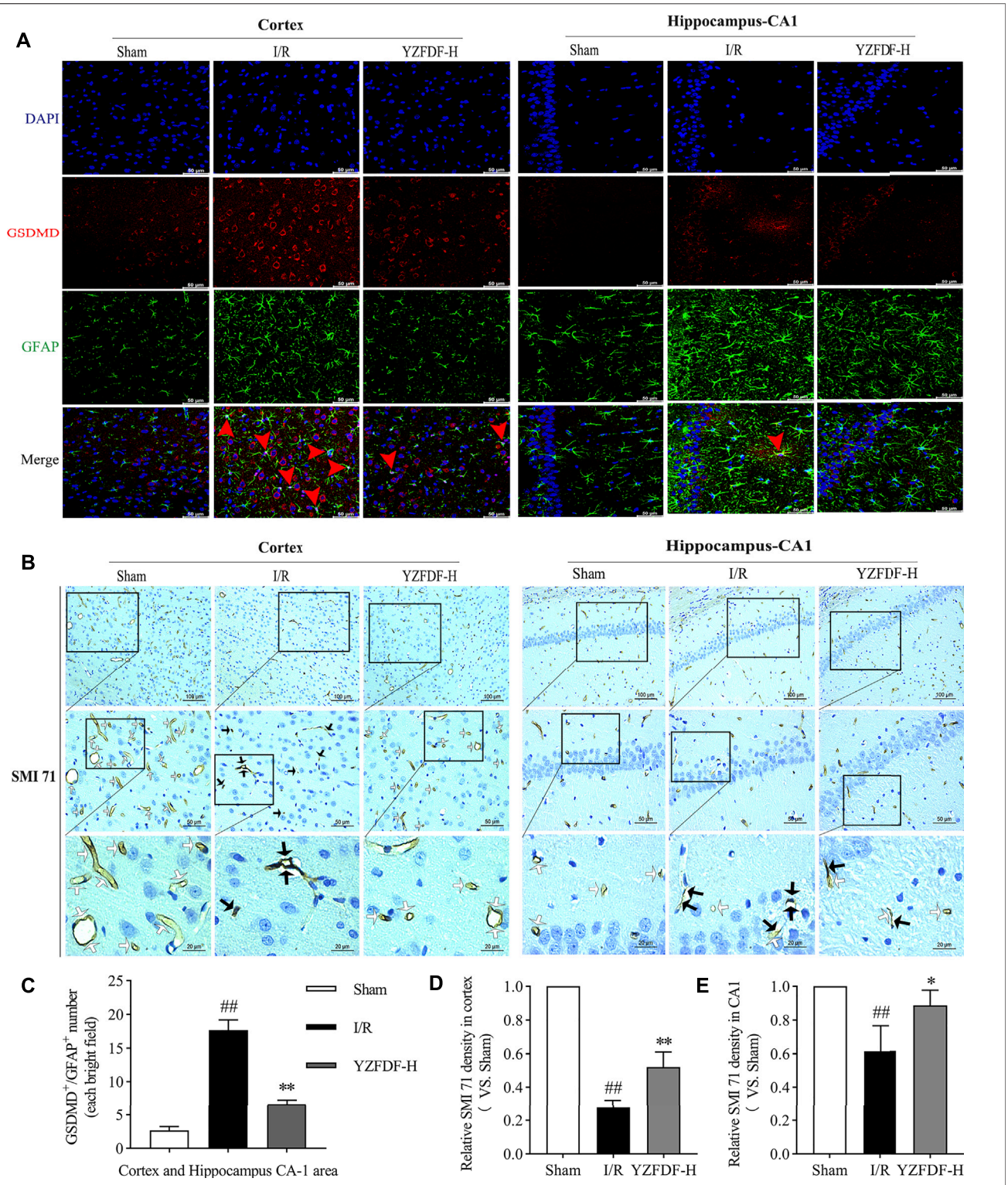

FIGURE 6 | YZFDF inhibited astrocytic pyroptosis and protected against BBB collapse at 24 h after cerebral I/R in rats. **(A)** Representative pictures of double immunofluorescence staining of GSDMD (red) with GFAP (green) in cortex and hippocampus-CA1 areas, scale bars = 50 μm. Red arrows show the GSDMD positive staining localized with the astrocytic nucleus. **(B)** Representative pictures of immunohistochemical staining of SMI 71 (a specific marker for BBB) in cortex and hippocampus-CA1 areas. White arrows show smooth and intact capillaries which represent normal BBB integrity, and black arrows indicate the damage of BBB integrity with unsmoothed, shriveled, or ruptured capillaries, scale bars = 100, 50, and 20 μm, as shown in pictures. **(C)** Quantitative analysis of astrocyte number with GSDMD-positive staining, $n = 3$. **(D)** Quantitative analysis of relative SMI 71 density in the cortex (scale bar = 50 μm), $n = 3$. **(E)** Quantitative analysis of relative SMI 71 density in the hippocampus-CA1 (scale bar = 50 μm), $n = 3$. $^{\#\#}p < 0.01$ vs. Sham group; $^{*}p < 0.05$, $^{**}p < 0.01$ vs. I/R group.

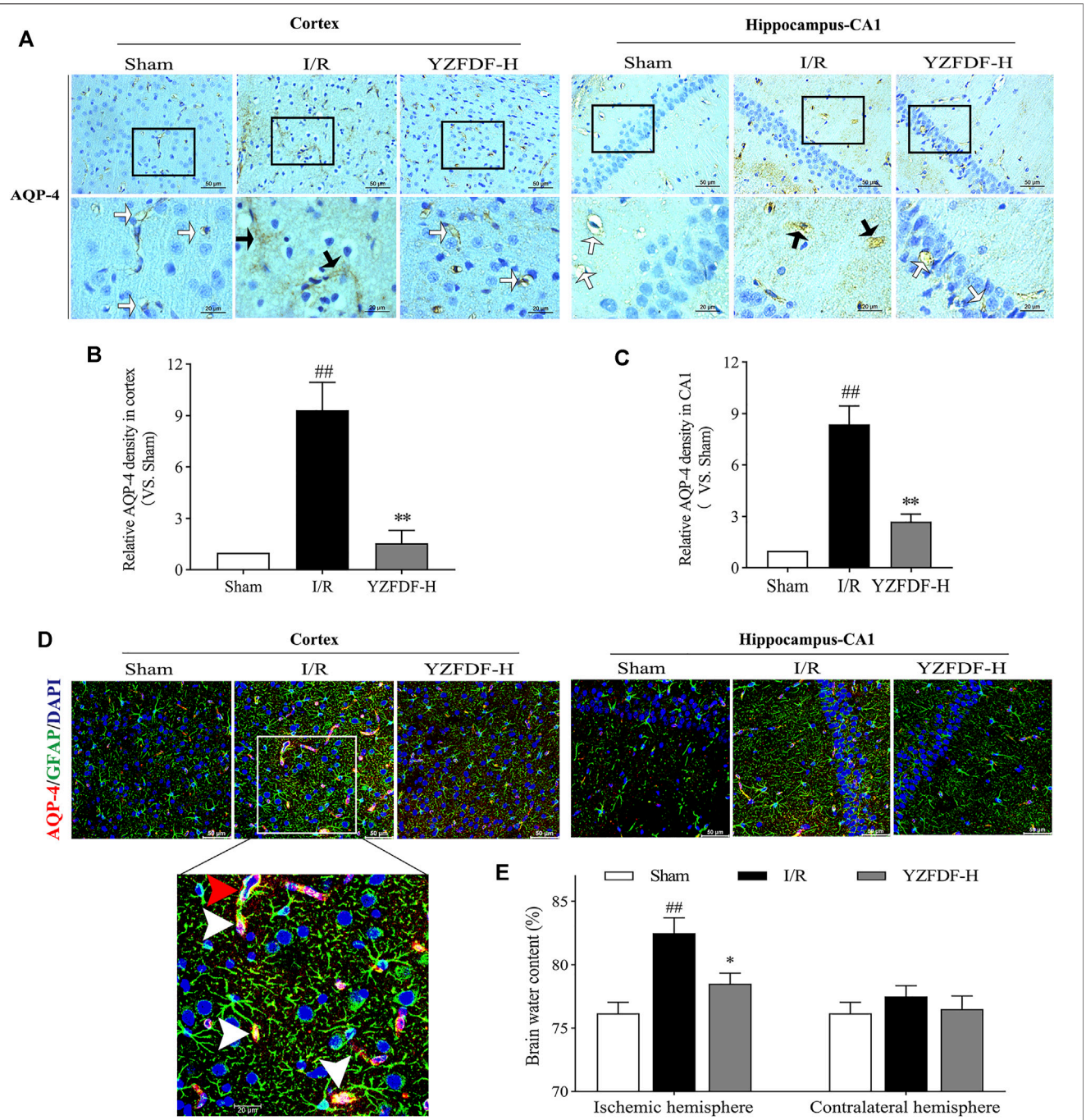

FIGURE 7 | YZFDF restored AQP-4 polarization and reduced astrocytic endfeet swelling and brain edema at 24 h after cerebral I/R in rats. **(A)** Representative pictures of immunohistochemical staining of AQP-4 in cortex and hippocampus-CA1 areas. White straight arrows represent normal AQP-4 polarization, and black arrows represent AQP-4 depolarization with obvious dispersion and perturbed expression, scale bars = 50 and 20 μm, as shown in pictures. **(B)** Quantitative analysis of relative AQP-4 density in the cortex (scale bar = 50 μm), $n = 3$. **(C)** Quantitative analysis of relative AQP-4 density in the hippocampus-CA1 (scale bar = 50 μm), $n = 3$. $^{\#\#}p < 0.01$ vs. Sham group; $^{**}p < 0.01$ vs. I/R group. **(D)** Representative pictures of double immunofluorescence staining of AQP-4 (red) with GFAP (green) in cortex and hippocampus-CA1 areas. Red triangle arrow indicates depolarized AQP-4 colocalizes with retracted GFAP and distributes around the astrocytic nucleus, and white triangle arrows indicate depolarized AQP-4 colocalizes with swelling of astrocytic endfeet, scale bars = 50 and 20 μm, as shown in pictures. **(E)** Brain water content analysis of ischemic and contralateral hemispheres, $n = 4$. $^{\#\#}p < 0.01$ vs. Sham group; $^{*}p < 0.05$ vs. I/R group.

onset and development of AD. However, accumulated evidence has showed that the neuroinflammation-related dysfunctional BBB–glymphatic system is responsible for triggering Aβ accumulation in the brain and may represent key link between ischemic stroke and dementia (Goulay et al., 2020; Ronaldson and Davis, 2020).

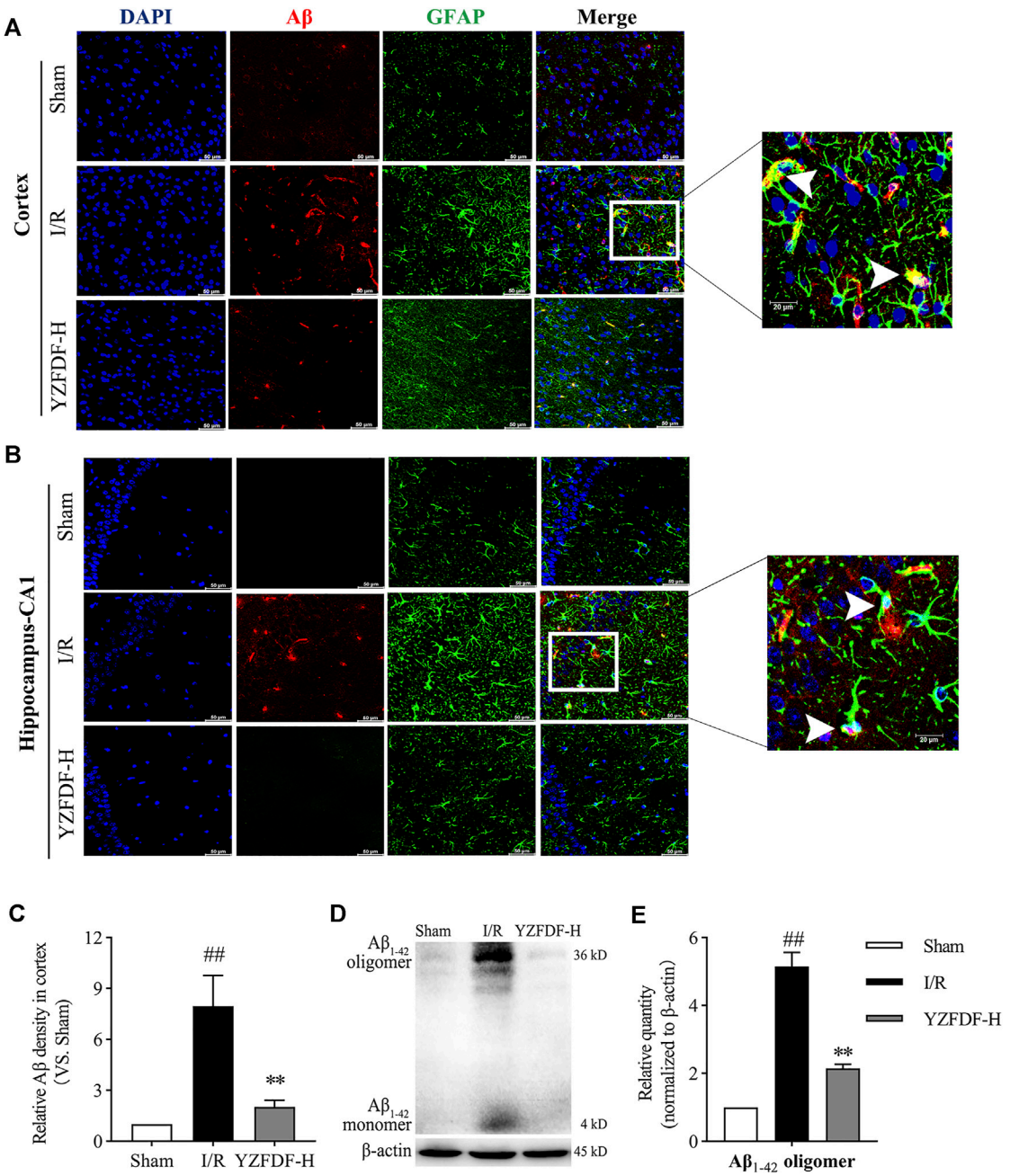

FIGURE 8 | YZFDF promoted Aβ clearance and prevented the formation of $A\beta_{1\text{-}42}$ oligomers at 24 h after cerebral I/R in rats. **(A,B)** Representative pictures of double immunofluorescence staining of Aβ (red) with GFAP (green) in cortex and hippocampus-CA1 areas, and white arrows represent Aβ accumulation in sites of swelling astrocytic endfeet, scale bars = 50 and 20 μm, as shown in pictures. **(C)** Quantitative analysis of relative Aβ density in the cortex (scale bar = 50 μm), $n = 3$. **(D)** Representative Western blots for the $A\beta_{1\text{-}42}$ monomer and $A\beta_{1\text{-}42}$ oligomer. **(E)** Quantitative analysis of $A\beta_{1\text{-}42}$ oligomers, $n = 6$. $^{\#\#}p < 0.01$ vs. Sham group; $^{**}p < 0.01$ vs. I/R group.

Restoring blood flow of the ischemic cerebral tissue in a short-time window is the most important therapeutic measure for patients suffering from acute cerebral ischemia. However, the potential additional injury following ischemia/reperfusion (I/R) has a great impact on the therapeutic efficacy of restoring blood flow (Kalogeris et al., 2016). I/R injury is the common pathophysiological phenomenon liable to occur in multiple organs including brain, and deterioration of microvasculature damage after reperfusion and the following non-reflow phenomenon of capillaries is the basic pathological change of I/R injury (Kloner et al., 2018). In the brain, the BBB is the main structure of microvasculature, and microcirculation disturbance resulting from BBB breakdown plays a crucial role in cerebral I/R injury (Mohamed Mokhtarudin and Payne, 2015; Huang et al., 2020; Xiao et al., 2020). Furthermore, BBB

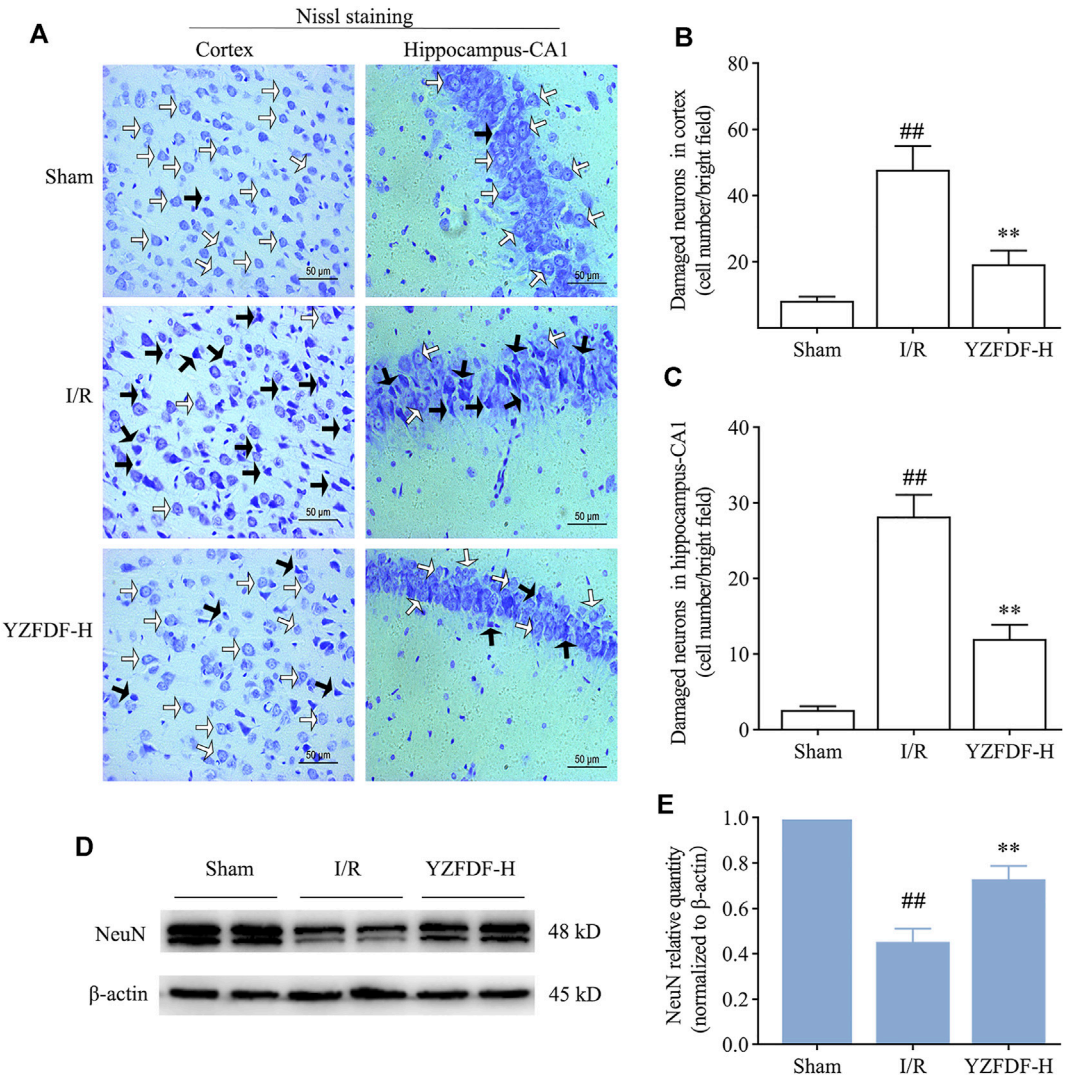

FIGURE 9 | YZFDF alleviated neuronal damage and promoted neuron survival at 24 h after cerebral I/R in rats. **(A)** Representative pictures of Nissl staining in ischemic cortex and hippocampus-CA1 areas. White arrows represent normal morphology of neurons with the clear nucleolus, abundant cytoplasm, and intact structure, and black arrows represent damaged neurons appearing shrunken and deep stained, scale bars = 50 μm. **(B,C)** Quantitative analysis of damaged neurons in cortex and hippocampus-CA1 areas, $n = 4$. $^{\#\#}p < 0.01$ vs. Sham group; $^{**}p < 0.01$ vs. I/R group. **(D)** Representative Western blots for NeuN. **(E)** Quantitative analysis of NeuN, $n = 6$. $^{\#\#}p < 0.01$ vs. Sham group; $^{**}p < 0.01$ vs. I/R group.

breakdown is recognized as an early marker for the onset of AD (Bell and Zlokovic, 2009; Sagare et al., 2012; Nation et al., 2019). Therefore, BBB protection during cerebral I/R injury is considered an important strategy for the prevention and treatment of ischemic stroke and poststroke dementia (Gursoy-Ozdemir et al., 2012; Goulay et al., 2020; Ronaldson and Davis, 2020).

As for the medication of cerebral I/R injury and BBB protection, amounts of literature indicated that various extracts or compound medicines from natural products show beneficial effects (Li Y. et al., 2019; Yu et al., 2020). For instance, Buyang Huanwu decoction (BHD) and Tongxinluo (TXL), both consisting of herbal and animal medicines, are common TCM prescriptions used for treating Qi deficiency and blood stasis syndrome of ischemic stroke by efficacies of invigorating Qi and activating blood circulation (Su et al., 2011; Wang Y. et al., 2020). Experimental studies revealed that BHD and TXL could alleviate cerebral I/R injury and exert protective effects on the BBB (Liu et al., 2013; Chen et al., 2019). In studies about the therapeutic efficacy of TCM compound medicines or extracts, such as BHD and TXL mentioned above for cerebral I/R injury, drug administration for 3–7 days starting before MCAO is the common means to enhance intervention effects (Liu et al., 2013; Yu et al., 2018; Chen et al., 2019; She et al., 2019; Zheng et al., 2019; Zhang S. et al., 2021). Accordingly, based on these literatures, we select YZFDF pretreatment to carry out the present study. However, different from BHD and TXL, YZFDF is purely composed of several plant-derived natural products, but the preliminary results in the present study showed that YZFDF could also exert significant neuroprotective effects against cerebral I/R injury by dose-

dependently alleviating neurological deficits and cerebral infarct after reperfusion. Our previous work revealed that pyroptosis of glial cells (microglia and astrocytes) is a considerable pathological mechanism causing BBB damage after cerebral I/R, and abating pyroptosis contributes to protect against BBB breakdown and maintains the homeostasis of brain microenvironments (Lyu et al., 2021). Our present study further indicated that YZFDF could protect ischemic cerebral tissues against pyroptotic cell death and accordingly exert protective effects against BBB collapse in damaged cortex and hippocampus areas after cerebral I/R, potentially promoting blood flow reperfusion in microcirculation of ischemic cerebral tissues, which probably owed to the multiple efficacies of invigorating Qi, removing blood stasis, and dredging brain collaterals.

As pro-inflammatory programmed cell death is distinguished from apoptosis and necrosis, pyroptosis manifests as nanopore formation on the cytomembrane leading to cell swelling and death, which is executed by the N-terminal fragments of gasdermin family represented by GSDMD-N (Feng et al., 2018). Upon stimulation, NLRP3 recruits pro-caspase-1 through the adapter molecule ASC to form the NLRP3/ASC/caspase-1 inflammasome, resulting in the activation of caspase-1 to cleave GSDMD and then leads to the secretion of pro-inflammatory cytokines, which is called canonical pyroptosis (Patel et al., 2017; Cong et al., 2020). However, in the caspase-11/GSDMD-mediated noncanonical pyroptosis pathway, GSDMD-N formed by the activation of caspase-11 acts as the upstream signaling that activates the NLRP3/ASC/caspase-1 inflammasome to further cause the maturation and secretion of pro-inflammatory cytokines such as IL-1β (Kayagaki et al., 2015; Aglietti et al., 2016). Caspase-11 is previously considered to be activated by lipopolysaccharide in infectious diseases (Hagar et al., 2013). Cerebral I/R injury is a noninfectious pathological process (Dong et al., 2018), and thus previous studies attributed cerebral I/R–induced pyroptosis to its canonical pathway (She et al., 2019). However, emerging literature has proven that caspase-11/GSDMD-mediated noncanonical pyroptosis is involved in acute kidney injury and hepatic injury induced by some endogenous pathophysiological factors including I/R injury (Miao et al., 2019; Wang X. et al., 2020). Our recent work revealed that caspase-11/GSDMD-mediated noncanonical pyroptosis also involves in cerebral I/R injury (Lyu et al., 2021). In the present study, we observed that YZFDF could obviously inactivate caspase-11 as well as cut off NLRP3/ASC/caspase-1 signaling and thus inhibit the cleavage of GSDMD to reduce the formation of GSDMD-N, indicating that YZFDF could exert inhibitory effects on cerebral I/R–induced canonical and noncanonical pyroptosis.

BBB breakdown in the cerebral ischemic period mainly results from the interaction between blood components (activated leukocytes and platelets) and microvascular endothelial cells, leading to inflammatory response and microthrombosis, which are exacerbated by blood flow reperfusion and then followed by the no-reflow phenomenon (Kalogeris et al., 2016). Following the initial ischemic damage, a wave of detrimental secondary events is caused by reperfusion such as oxidative stress and acute inflammation. Because inflammatory response is inherent across the whole course of cerebral I/R injury, and additionally due to the exacerbation of thromboinflammation and no-reflow after reperfusion in capillaries, neuroinflammation is recognized as the most vital pathological factor impacting on the BBB and the fundamental therapeutic target during both ischemic period and reperfusion (Liu et al., 2014; Li WH. et al., 2019; Stoll and Nieswandt, 2019). The results in our present study showed that YZFDF pretreatment could obviously downregulate the levels of IL-6 and inhibit the aberrant activation of microglia, reflecting that YZFDF alleviated the acute neuroinflammation during the course of cerebral I/R. There are intimate relationships between inflammation and pyroptosis (Kesavardhana et al., 2020). Research has proven that infectious or sterile inflammation can stimulate occurrence of pyroptosis, while pyroptosis reversely aggravates inflammatory responses by further generating and releasing certain pro-inflammatory mediators (Patel et al., 2017). In present study, our results further indicated that YZFDF could exert obvious inhibitory effects on microglial pyroptosis and the generation of IL-1β, which provided evidence for the blocking effect of YZFDF on cross talks between neuroinflammation and pyroptosis after reperfusion.

In addition to microglia, astrocytes are as well the main locations of cerebral I/R–induced pyroptosis which peaks at 24 h after reperfusion (Zhang et al., 2019; Lyu et al., 2021). As the most abundant glial cells in the mammalian brain, astrocytes are the major supporter of energy supply and nutrition for neurons in neuro-glial-vascular coupling (Nortley and Attwell, 2017; Allen and Lyons, 2018), and moreover astrocytic endfeet function as essential components of both the BBB and glymphatic system to clear metabolites such as Aβ and maintain brain microenvironmental homeostasis, in which aquaporin-4 (AQP-4) on astrocytic endfeet plays an important role (Gleiser et al., 2016; Rasmussen et al., 2021). Thus, in our previous study (Lyu et al., 2021), astrocytic pyroptosis was considered a vital factor causing the BBB further disruption and AQP-4 polarization loss, which account for Aβ accumulation, brain edema formation, non-reflow phenomenon of capillaries, and neuronal damage after cerebral I/R. In the present study, our results showed that YZFDF could obviously inhibit astrocytic pyroptosis after reperfusion which contributed to restore AQP-4 polarization and reduce brain edema. Moreover, the results as well showed that based on the protective effects against BBB–glymphatic dysfunctions, YZFDF could further significantly promote Aβ clearance and prevented the formation of $A\beta_{1\text{-}42}$ oligomers after reperfusion.

Aβ accumulation is the essential factor in the biological definition of AD, which can further cause tau pathology and neuron loss (Jack et al., 2018). Furthermore, Aβ accumulation in the brain can lead to extensive damages of the neurovascular unit (NVU) which comprises neurons, perivascular microglia, and BBB including cerebral microvascular endothelial cells (CMECs), pericytes, and surrounding astrocytes (Yamazaki and Kanekiyo, 2017). As mentioned previously, accumulated Aβ can act on pericytes via evoking reactive oxygen species generation in the form of oligomers to constrict capillaries which further promotes energy lack of neurons and neurodegeneration (Nortley et al., 2019). Aβ accumulation in capillaries, associated with cerebral amyloid angiopathy (CAA), also affect NVU astrocytes to cause mislocalization of AQP-4 expression (Wilcock et al., 2009), which was consistent with the acute accumulation of Aβ around swelling astrocytic endfeet as shown in our present study. Our previous study indicated that $A\beta_{1\text{-}42}$ oligomers are the main form of toxic Aβ and that $A\beta_{1\text{-}42}$ oligomers could damage tight junction scaffold proteins

among CMECs to induce BBB leakage via the receptor for advanced glycation end product (RAGE) (Wan W. et al., 2014; Wan et al., 2015; Chan et al., 2018; Chen et al., 2018). Previous studies demonstrated that Aβ increasingly accumulates around astrocytes along with both BBB breakdown and delayed neuronal death in the hippocampus within 6 months after cerebral I/R and even deposits as plaques with time further extension (van Groen et al., 2005; Pluta et al., 2010), which provides experimental evidence for stroke-inducing sporadic AD. Furthermore, recently, Martins et al. revealed that Aβ oligomers potentially resulting from activated platelets in microthrombosis massively accumulate in brain tissues including capillaries within 24 h after cerebral I/R, and they further demonstrated that Aβ oligomers are responsible for some of the brain damage during stroke by the property of forming ion channels on the cytomembrane (in a non-receptor–dependent way) to affect cellular osmotic balance and promote brain edema formation (Martins et al., 2019). Our recent study revealed that pyroptosis accounts for dysfunctions of the BBB–glymphatic system and the acute accumulation of toxic Aβ within 24 h after cerebral I/R (Lyu et al., 2021). However, on the other hand, toxic Aβ has been identified as a cause of pyroptosis and neuroinflammation in previous studies (Halle et al., 2008; Shi F. et al., 2015), which suggests a magnified effect of Aβ accumulation after cerebral I/R.

Large amounts of evidence mentioned previously indicate that Aβ accumulation is not only the consequence but also the further cause of the dysfunctional BBB–glymphatic system and neuronal damage in the course of cerebral I/R injury and in the process of ischemic stroke–inducing dementia. Therefore, maintaining Aβ clearance and protecting brain tissues against Aβ toxicity after cerebral I/R could offer a new viewpoint to alleviate ischemic stroke and prevent poststroke dementia. TCM herbal formulas or extracts have shown unique advantages in the prevention and treatment of complex brain diseases including acute ischemic stroke and dementia (Li Y. et al., 2019; Yu et al., 2020). Our previous study demonstrated that YZFDF could exert protective effects against $A\beta_{1\text{-}42}$ oligomer–induced BBB and neuronal damages (Liu et al., 2016a; Chan et al., 2020). The present study showed that YZFDF could promote Aβ clearance to prevent Aβ acute accumulation and the formation of $A\beta_{1\text{-}42}$ oligomers and thus block the potential interaction between the BBB–glymphatic dysfunctions and Aβ accumulation. Viewed from the macro perspective of TCM holism, the four herbal medicines of YZFDF potentially possess the neuroprotective effects against cerebral I/R injury by synergistically exerting efficacies of invigorating Qi, removing blood stasis, and dredging brain collaterals based on their drug properties. From the modern pharmacological and microcosmic perspective, our previous study had identified the bioactive ingredients in YZFDF, which contain bilobalide and ginkgolide A of *Ginkgo biloba* leaves, ginsenoside Rg1 of ginseng, cistanoside A of Cistanches Herba, and α-asarone of grassleaf sweetflag, which have a wide range of activities including anti-inflammation, anti-aggregation of platelets and proteins, neurovascular protections, and neurotrophic effects against cerebral I/R injury (Kimura et al., 1988; Zhou et al., 2014; Liu et al., 2016a; Zheng et al., 2019; Sarkar et al., 2020; Zhang K. et al., 2021). Our previous studies indicated that EGb761, a product extracted from *Ginkgo biloba* leaves (the main herb of YZFDF), could regulate Aβ-induced microglial inflammatory responses, BBB disruption, and alleviate neuronal damage (Wan WB. et al., 2014; Liu et al., 2016b; Wan et al., 2016). As a consequence, in this study, YZFDF potentially exerted advantages of multiple bioactive ingredients, multiple effects, and multiple targets on the whole NVU to alleviate cerebral I/R–induced neuroinflammation, pyroptosis, BBB–glymphatic dysfunctions, Aβ accumulation, and their interactions. Nevertheless, the action on body systems of YZFDF in this study and post-treatment and long-term effects as well as the more detailed targets and mechanism remain to be clarified and deserve our further explorations in future research.

CONCLUSION

In summary, we demonstrated the neuroprotective properties of YZFDF against cerebral I/R injury at the first stage, and the following study further indicated that YZFDF pretreatment could exert inhibitory effects on microglial and astrocytic pyroptosis and acute neuroinflammation, which fundamentally contribute to restore the BBB–glymphatic functions, promote Aβ clearance and prevent the formation of Aβ oligomers via protecting against BBB breakdown, and AQP-4 polarization loss and thus facilitates to maintain the homeostasis of brain microenvironments and neuron survival after cerebral I/R.

DATA AVAILABILITY STATEMENT

The original contributions presented in the study are included in the article/**Supplementary Material**, further inquiries can be directed to the corresponding authors.

ETHICS STATEMENT

The animal study was reviewed and approved by the Animal Care Committee of Shanghai Jiao Tong University Affiliated Sixth People's Hospital.

AUTHOR CONTRIBUTIONS

YL and CZ conceived and designed the project. ZL, QL, and ZY performed the experiments, analyzed the data, and wrote the manuscript. YC and LF contributed to assist the implementation of experiments. All authors read and approved the final manuscript.

FUNDING

This work was supported by the National Natural Science Foundation of China (Grant Nos 81473739 and 81703857).

SUPPLEMENTARY MATERIAL

The Supplementary Material for this article can be found online at: https://www.frontiersin.org/articles/10.3389/fphar.2021.791059/full#supplementary-material

REFERENCES

Aglietti, R. A., Estevez, A., Gupta, A., Ramirez, M. G., Liu, P. S., Kayagaki, N., et al. (2016). GsdmD P30 Elicited by Caspase-11 during Pyroptosis Forms Pores in Membranes. *Proc. Natl. Acad. Sci. U S A.* 113 (28), 7858–7863. doi:10.1073/pnas.1607769113

Allen, N. J., and Lyons, D. A. (2018). Glia as Architects of central Nervous System Formation and Function. *Science* 362 (6411), 181–185. doi:10.1126/science.aat0473

Alzheimer's Association (2021). 2021 Alzheimer's Disease Facts and Figures. *Alzheimers Dement* 17 (3), 327–406. doi:10.1002/alz.12328

Bell, R. D., and Zlokovic, B. V. (2009). Neurovascular Mechanisms and Blood-Brain Barrier Disorder in Alzheimer's Disease. *Acta Neuropathol.* 118 (1), 103–113. doi:10.1007/s00401-009-0522-3

Burrows, F., Haley, M. J., Scott, E., Coutts, G., Lawrence, C. B., Allan, S. M., et al. (2016). Systemic Inflammation Affects Reperfusion Following Transient Cerebral Ischaemia. *Exp. Neurol.* 277, 252–260. doi:10.1016/j.expneurol.2016.01.013

Cai, M., Yu, Z., Wang, L., Song, X., Zhang, J., Zhang, Z., et al. (2016). Tongxinluo Reduces Brain Edema and Inhibits post-ischemic Inflammation after Middle Cerebral Artery Occlusion in Rats. *J. Ethnopharmacol* 181, 136–145. doi:10.1016/j.jep.2016.01.026

Carbone, M. G., Pagni, G., Tagliarini, C., Imbimbo, B. P., and Pomara, N. (2021). Can Platelet Activation Result in Increased Plasma Aβ Levels and Contribute to the Pathogenesis of Alzheimer's Disease? *Ageing Res. Rev.* 71, 101420. doi:10.1016/j.arr.2021.101420

Cavallucci, V., D'Amelio, M., and Cecconi, F. (2012). Aβ Toxicity in Alzheimer's Disease. *Mol. Neurobiol.* 45 (2), 366–378. doi:10.1007/s12035-012-8251-3

Chan, Y., Chen, W., Chen, Y., Lv, Z., Wan, W., Li, Y., et al. (2020). Yi-Zhi-Fang-Dai Formula Exerts a Protective Effect on the Injury of Tight Junction Scaffold Proteins *In Vitro* and *In Vivo* by Mediating Autophagy through Regulation of the RAGE/CaMKKβ/AMPK/mTOR Pathway. *Biol. Pharm. Bull.* 43 (12), 1847–1858. doi:10.1248/bpb.b20-00379

Chan, Y., Chen, W., Wan, W., Chen, Y., Li, Y., and Zhang, C. (2018). Aβ1-42 Oligomer Induces Alteration of Tight junction Scaffold Proteins via RAGE-Mediated Autophagy in bEnd.3 Cells. *Exp. Cel Res* 369 (2), 266–274. doi:10.1016/j.yexcr.2018.05.025

Chen, W., Chan, Y., Wan, W., Li, Y., and Zhang, C. (2018). Aβ1-42 Induces Cell Damage via RAGE-dependent Endoplasmic Reticulum Stress in bEnd.3 Cells. *Exp. Cel Res* 362 (1), 83–89. doi:10.1016/j.yexcr.2017.11.005

Chen, Z. Z., Gong, X., Guo, Q., Zhao, H., and Wang, L. (2019). Bu Yang Huan Wu Decoction Prevents Reperfusion Injury Following Ischemic Stroke in Rats via Inhibition of HIF-1 α, VEGF and Promotion β-ENaC Expression. *J. Ethnopharmacol* 228, 70–81. doi:10.1016/j.jep.2018.09.017

Cong, L., Gao, Z., Zheng, Y., Ye, T., Wang, Z., Wang, P., et al. (2020). Electrical Stimulation Inhibits Val-boroPro-Induced Pyroptosis in THP-1 Macrophages via Sirtuin3 Activation to Promote Autophagy and Inhibit ROS Generation. *Aging (Albany NY)* 12 (7), 6415–6435. doi:10.18632/aging.103038

Dong, Z., Pan, K., Pan, J., Peng, Q., and Wang, Y. (2018). The Possibility and Molecular Mechanisms of Cell Pyroptosis after Cerebral Ischemia. *Neurosci. Bull.* 34 (6), 1131–1136. doi:10.1007/s12264-018-0294-7

Du, H., He, Y., Pan, Y., Zhao, M., Li, Z., Wang, Y., et al. (2021). Danhong Injection Attenuates Cerebral Ischemia-Reperfusion Injury in Rats through the Suppression of the Neuroinflammation. *Front. Pharmacol.* 12, 561237. doi:10.3389/fphar.2021.561237

Eskandari, S., Sajadimajd, S., Alaei, L., Soheilikhah, Z., Derakhshankhah, H., and Bahrami, G. (2021). Targeting Common Signaling Pathways for the Treatment of Stroke and Alzheimer's: a Comprehensive Review. *Neurotox Res.* 39 (5), 1589–1612. doi:10.1007/s12640-021-00381-7

Feng, S., Fox, D., and Man, S. M. (2018). Mechanisms of Gasdermin Family Members in Inflammasome Signaling and Cell Death. *J. Mol. Biol.* 430 (18 Pt B), 3068–3080. doi:10.1016/j.jmb.2018.07.002

Gleiser, C., Wagner, A., Fallier-Becker, P., Wolburg, H., Hirt, B., and Mack, A. F. (2016). Aquaporin-4 in Astroglial Cells in the CNS and Supporting Cells of Sensory Organs-A Comparative Perspective. *Int. J. Mol. Sci.* 17 (9), 1411. doi:10.3390/ijms17091411

Goulay, R., Mena Romo, L., Hol, E. M., and Dijkhuizen, R. M. (2020). From Stroke to Dementia: a Comprehensive Review Exposing Tight Interactions between Stroke and Amyloid-β Formation. *Transl Stroke Res.* 11 (4), 601–614. doi:10.1007/s12975-019-00755-2

Gursoy-Ozdemir, Y., Yemisci, M., and Dalkara, T. (2012). Microvascular protection Is Essential for Successful Neuroprotection in Stroke. *J. Neurochem.* 123 (Suppl. 2), 2–11. doi:10.1111/j.1471-4159.2012.07938.x

Hagar, J. A., Powell, D. A., Aachoui, Y., Ernst, R. K., and Miao, E. A. (2013). Cytoplasmic LPS Activates Caspase-11: Implications in TLR4-independent Endotoxic Shock. *Science* 341 (6151), 1250–1253. doi:10.1126/science.1240988

Halle, A., Hornung, V., Petzold, G. C., Stewart, C. R., Monks, B. G., Reinheckel, T., et al. (2008). The NALP3 Inflammasome Is Involved in the Innate Immune Response to Amyloid-Beta. *Nat. Immunol.* 9 (8), 857–865. doi:10.1038/ni.1636

Hampel, H., Hardy, J., Blennow, K., Chen, C., Perry, G., Kim, S. H., et al. (2021). The Amyloid-β Pathway in Alzheimer's Disease. *Mol. Psychiatry*. doi:10.1038/s41380-021-01249-0

Huang, Y., Chen, S., Luo, Y., and Han, Z. (2020). Crosstalk between Inflammation and the BBB in Stroke. *Curr. Neuropharmacol* 18 (12), 1227–1236. doi:10.2174/1570159X18666200620230321

Hussain, B., Fang, C., and Chang, J. (2021). Blood-Brain Barrier Breakdown: An Emerging Biomarker of Cognitive Impairment in Normal Aging and Dementia. *Front. Neurosci.* 15, 688090. doi:10.3389/fnins.2021.688090

Jack, C. R., Jr., Bennett, D. A., Blennow, K., Carrillo, M. C., Dunn, B., Haeberlein, S. B., et al. (2018). NIA-AA Research Framework: Toward a Biological Definition of Alzheimer's Disease. *Alzheimers Dement* 14 (4), 535–562. doi:10.1016/j.jalz.2018.02.018

Kalogeris, T., Baines, C. P., Krenz, M., and Korthuis, R. J. (2016). Ischemia/Reperfusion. *Compr. Physiol.* 7 (1), 113–170. doi:10.1002/cphy.c160006

Kayagaki, N., Stowe, I. B., Lee, B. L., O'Rourke, K., Anderson, K., Warming, S., et al. (2015). Caspase-11 Cleaves Gasdermin D for Non-canonical Inflammasome Signalling. *Nature* 526 (7575), 666–671. doi:10.1038/nature15541

Kesavardhana, S., Malireddi, R. K. S., and Kanneganti, T. D. (2020). Caspases in Cell Death, Inflammation, and Pyroptosis. *Annu. Rev. Immunol.* 38, 567–595. doi:10.1146/annurev-immunol-073119-095439

Kim, D., Hughes, T. M., Lipford, M. E., Craft, S., Baker, L. D., Lockhart, S. N., et al. (2021). Relationship between Cerebrovascular Reactivity and Cognition Among People with Risk of Cognitive Decline. *Front. Physiol.* 12, 645342. doi:10.3389/fphys.2021.645342

Kimura, Y., Okuda, H., and Arichi, S. (1988). Effects of Various Ginseng Saponins on 5-hydroxytryptamine Release and Aggregation in Human Platelets. *J. Pharm. Pharmacol.* 40 (12), 838–843. doi:10.1111/j.2042-7158.1988.tb06285.x

Kloner, R. A., King, K. S., and Harrington, M. G. (2018). No-reflow Phenomenon in the Heart and Brain. *Am. J. Physiol. Heart Circ. Physiol.* 315 (3), H550–H562. doi:10.1152/ajpheart.00183.2018

Lan, R., Xiang, J., Wang, G. H., Li, W. W., Zhang, W., Xu, L. L., et al. (2013). Xiao-Xu-Ming Decoction Protects against Blood-Brain Barrier Disruption and Neurological Injury Induced by Cerebral Ischemia and Reperfusion in Rats. *Evid. Based Complement. Alternat Med.* 2013, 629782. doi:10.1155/2013/629782

Li, W. H., Cheng, X., Yang, Y. L., Liu, M., Zhang, S. S., Wang, Y. H., et al. (2019a). Kaempferol Attenuates Neuroinflammation and Blood Brain Barrier Dysfunction to Improve Neurological Deficits in Cerebral Ischemia/reperfusion Rats. *Brain Res.* 1722, 146361. doi:10.1016/j.brainres.2019.146361

Li, Y., Zhong, W., Jiang, Z., and Tang, X. (2019b). New Progress in the Approaches for Blood-Brain Barrier protection in Acute Ischemic Stroke. *Brain Res. Bull.* 144, 46–57. doi:10.1016/j.brainresbull.2018.11.006

Liu, L., Wan, W., Chen, W., Chan, Y., Shen, Q., and Li, Y. (2016a). Yi-Zhi-Fang-Dai Formula Protects against Aβ1-42 Oligomer Induced Cell Damage via Increasing Hsp70 and Grp78 Expression in SH-Sy5y Cells. *Evid. Based Complement. Alternat Med.* 2016, 8591656. doi:10.1155/2016/8591656

Liu, L., Zhang, C., Kalionis, B., Wan, W., Murthi, P., Chen, C., et al. (2016b). EGb761 Protects against Aβ1-42 Oligomer-Induced Cell Damage via Endoplasmic Reticulum Stress Activation and Hsp70 Protein Expression Increase in SH-Sy5y Cells. *Exp. Gerontol.* 75, 56–63. doi:10.1016/j.exger.2016.01.003

Liu, T., Zhang, T., Yu, H., Shen, H., and Xia, W. (2014). Adjudin Protects against Cerebral Ischemia Reperfusion Injury by Inhibition of Neuroinflammation and

Blood-Brain Barrier Disruption. *J. Neuroinflammation* 11, 107. doi:10.1186/1742-2094-11-107

Liu, W., Wong, A., Au, L., Yang, J., Wang, Z., Leung, E. Y., et al. (2015). Influence of Amyloid-β on Cognitive Decline after Stroke/Transient Ischemic Attack: Three-Year Longitudinal Study. *Stroke* 46 (11), 3074–3080. doi:10.1161/STROKEAHA.115.010449

Liu, Y., Tang, G. H., Sun, Y. H., Lin, X. J., Wei, C., Yang, G. Y., et al. (2013). The Protective Role of Tongxinluo on Blood-Brain Barrier after Ischemia-Reperfusion Brain Injury. *J. Ethnopharmacol* 148 (2), 632–639. doi:10.1016/j.jep.2013.05.018

Longa, E. Z., Weinstein, P. R., Carlson, S., and Cummins, R. (1989). Reversible Middle Cerebral Artery Occlusion without Craniectomy in Rats. *Stroke* 20 (1), 84–91. doi:10.1161/01.str.20.1.84

Lyu, Z., Chan, Y., Li, Q., Zhang, Q., Liu, K., Xiang, J., et al. (2021). Destructive Effects of Pyroptosis on Homeostasis of Neuron Survival Associated with the Dysfunctional BBB-Glymphatic System and Amyloid-Beta Accumulation after Cerebral Ischemia/Reperfusion in Rats. *Neural Plast.* 2021, 4504363. doi:10.1155/2021/4504363

Martins, A. H., Zayas-Santiago, A., Ferrer-Acosta, Y., Martinez-Jimenez, S. M., Zueva, L., Diaz-Garcia, A., et al. (2019). Accumulation of Amyloid Beta (Aβ) Peptide on Blood Vessel Walls in the Damaged Brain after Transient Middle Cerebral Artery Occlusion. *Biomolecules* 9 (8), 350. doi:10.3390/biom9080350

Matikainen, S., Nyman, T. A., and Cypryk, W. (2020). Function and Regulation of Noncanonical Caspase-4/5/11 Inflammasome. *J. Immunol.* 204 (12), 3063–3069. doi:10.4049/jimmunol.2000373

Merlini, M., Meyer, E. P., Ulmann-Schuler, A., and Nitsch, R. M. (2011). Vascular β-amyloid and Early Astrocyte Alterations Impair Cerebrovascular Function and Cerebral Metabolism in Transgenic arcAβ Mice. *Acta Neuropathol.* 122 (3), 293–311. doi:10.1007/s00401-011-0834-y

Miao, N., Yin, F., Xie, H., Wang, Y., Xu, Y., Shen, Y., et al. (2019). The Cleavage of Gasdermin D by Caspase-11 Promotes Tubular Epithelial Cell Pyroptosis and Urinary IL-18 Excretion in Acute Kidney Injury. *Kidney Int.* 96 (5), 1105–1120. doi:10.1016/j.kint.2019.04.035

Mohamed Mokhtarudin, M. J., and Payne, S. J. (2015). Mathematical Model of the Effect of Ischemia-Reperfusion on Brain Capillary Collapse and Tissue Swelling. *Math. Biosci.* 263, 111–120. doi:10.1016/j.mbs.2015.02.011

Nakada, T., Kwee, I. L., Igarashi, H., and Suzuki, Y. (2017). Aquaporin-4 Functionality and Virchow-Robin Space Water Dynamics: Physiological Model for Neurovascular Coupling and Glymphatic Flow. *Int. J. Mol. Sci.* 18 (8), 1798. doi:10.3390/ijms18081798

Nation, D. A., Sweeney, M. D., Montagne, A., Sagare, A. P., D'Orazio, L. M., Pachicano, M., et al. (2019). Blood-brain Barrier Breakdown Is an Early Biomarker of Human Cognitive Dysfunction. *Nat. Med.* 25 (2), 270–276. doi:10.1038/s41591-018-0297-y

Nortley, R., and Attwell, D. (2017). Control of Brain Energy Supply by Astrocytes. *Curr. Opin. Neurobiol.* 47, 80–85. doi:10.1016/j.conb.2017.09.012

Nortley, R., Korte, N., Izquierdo, P., Hirunpattarasilp, C., Mishra, A., Jaunmuktane, Z., et al. (2019). Amyloid β Oligomers Constrict Human Capillaries in Alzheimer's Disease via Signaling to Pericytes. *Science* 365 (6450). doi:10.1126/science.aav9518

Patel, M. N., Carroll, R. G., Galván-Peña, S., Mills, E. L., Olden, R., Triantafilou, M., et al. (2017). Inflammasome Priming in Sterile Inflammatory Disease. *Trends Mol. Med.* 23 (2), 165–180. doi:10.1016/j.molmed.2016.12.007

Pluta, R., Januszewski, S., Jabłoński, M., and Ułamek, M. (2010). Factors in Creepy Delayed Neuronal Death in hippocampus Following Brain Ischemia-Reperfusion Injury with Long-Term Survival. *Acta Neurochir Suppl.* 106, 37–41. doi:10.1007/978-3-211-98811-4_5

Rasmussen, M. K., Mestre, H., and Nedergaard, M. (2021). Fluid Transport in the Brain. *Physiol. Rev.* doi:10.1152/physrev.00031.2020

Ronaldson, P. T., and Davis, T. P. (2020). Regulation of Blood-Brain Barrier Integrity by Microglia in Health and Disease: A Therapeutic Opportunity. *J. Cereb. Blood Flow Metab.* 40 (1_Suppl. l), S6–S24. doi:10.1177/0271678X20951995

Sagare, A. P., Bell, R. D., and Zlokovic, B. V. (2012). Neurovascular Dysfunction and Faulty Amyloid β-peptide Clearance in Alzheimer Disease. *Cold Spring Harb Perspect. Med.* 2 (10), a011452. doi:10.1101/cshperspect.a011452

Sarkar, C., Quispe, C., Jamaddar, S., Hossain, R., Ray, P., Mondal, M., et al. (2020). Therapeutic Promises of Ginkgolide A: A Literature-Based Review. *Biomed. Pharmacother.* 132, 110908. doi:10.1016/j.biopha.2020.110908

She, Y., Shao, L., Zhang, Y., Hao, Y., Cai, Y., Cheng, Z., et al. (2019). Neuroprotective Effect of Glycosides in Buyang Huanwu Decoction on Pyroptosis Following Cerebral Ischemia-Reperfusion Injury in Rats. *J. Ethnopharmacol* 242, 112051. doi:10.1016/j.jep.2019.112051

Shi, F., Kouadir, M., and Yang, Y. (2015a). NALP3 Inflammasome Activation in Protein Misfolding Diseases. *Life Sci.* 135, 9–14. doi:10.1016/j.lfs.2015.05.011

Shi, J., Zhao, Y., Wang, K., Shi, X., Wang, Y., Huang, H., et al. (2015b). Cleavage of GSDMD by Inflammatory Caspases Determines Pyroptotic Cell Death. *Nature* 526 (7575), 660–665. doi:10.1038/nature15514

Singh, A. K., Rai, S. N., Maurya, A., Mishra, G., Awasthi, R., Shakya, A., et al. (2021). Therapeutic Potential of Phytoconstituents in Management of Alzheimer's Disease. *Evid. Based Complement. Alternat Med.* 2021, 5578574. doi:10.1155/2021/5578574

Song, B., Ao, Q., Niu, Y., Shen, Q., Zuo, H., Zhang, X., et al. (2013). Amyloid Beta-Peptide Worsens Cognitive Impairment Following Cerebral Ischemia-Reperfusion Injury. *Neural Regen. Res.* 8 (26), 2449–2457. doi:10.3969/j.issn.1673-5374.2013.26.006

Stoll, G., and Nieswandt, B. (2019). Thrombo-inflammation in Acute Ischaemic Stroke - Implications for Treatment. *Nat. Rev. Neurol.* 15 (8), 473–481. doi:10.1038/s41582-019-0221-1

Su, L., Li, Y., Lv, B., Ji, H., Ding, H., Hu, L., et al. (2011). Clinical Study on Naoxintong Capsule for Stroke Recovery of Qi-Deficiency and Blood-Stasis Syndrome. *Zhongguo Zhong Yao Za Zhi* 36 (11), 1530–1533.

Tarasoff-Conway, J. M., Carare, R. O., Osorio, R. S., Glodzik, L., Butler, T., Fieremans, E., et al. (2015). Clearance Systems in the Brain-Implications for Alzheimer Disease. *Nat. Rev. Neurol.* 11 (8), 457–470. doi:10.1038/nrneurol.2015.119

van Groen, T., Puurunen, K., Mäki, H. M., Sivenius, J., and Jolkkonen, J. (2005). Transformation of Diffuse Beta-Amyloid Precursor Protein and Beta-Amyloid Deposits to Plaques in the Thalamus after Transient Occlusion of the Middle Cerebral Artery in Rats. *Stroke* 36 (7), 1551–1556. doi:10.1161/01.STR.0000169933.88903.cf

Verheggen, I. C. M., Van Boxtel, M. P. J., Verhey, F. R. J., Jansen, J. F. A., and Backes, W. H. (2018). Interaction between Blood-Brain Barrier and Glymphatic System in Solute Clearance. *Neurosci. Biobehav Rev.* 90, 26–33. doi:10.1016/j.neubiorev.2018.03.028

Wan, W., Cao, L., Liu, L., Zhang, C., Kalionis, B., Tai, X., et al. (2015). Aβ(1-42) Oligomer-Induced Leakage in an *In Vitro* Blood-Brain Barrier Model Is Associated with Up-Regulation of RAGE and Metalloproteinases, and Down-Regulation of Tight junction Scaffold Proteins. *J. Neurochem.* 134 (2), 382–393. doi:10.1111/jnc.13122

Wan, W., Chen, H., and Li, Y. (2014a). The Potential Mechanisms of Aβ-Receptor for Advanced Glycation End-Products Interaction Disrupting Tight Junctions of the Blood-Brain Barrier in Alzheimer's Disease. *Int. J. Neurosci.* 124 (2), 75–81. doi:10.3109/00207454.2013.825258

Wan, W., Zhang, C., Danielsen, M., Li, Q., Chen, W., Chan, Y., et al. (2016). EGb761 Improves Cognitive Function and Regulates Inflammatory Responses in the APP/PS1 Mouse. *Exp. Gerontol.* 81, 92–100. doi:10.1016/j.exger.2016.05.007

Wan, W. B., Cao, L., Liu, L. M., Kalionis, B., Chen, C., Tai, X. T., et al. (2014b). EGb761 Provides a Protective Effect against Aβ1-42 Oligomer-Induced Cell Damage and Blood-Brain Barrier Disruption in an *In Vitro* bEnd.3 Endothelial Model. *PLoS One* 9 (11), e113126. doi:10.1371/journal.pone.0113126

Wang, B., Lyu, Z., Chan, Y., Li, Q., Zhang, L., Liu, K., et al. (2021a). Tongxinluo Exerts Inhibitory Effects on Pyroptosis and Amyloid-β Peptide Accumulation after Cerebral Ischemia/Reperfusion in Rats. *Evid. Based Complement. Alternat Med.* 2021, 5788602. doi:10.1155/2021/5788602

Wang, R., Qiu, C., Dintica, C. S., Shang, Y., Calderón Larrañaga, A., Wang, H. X., et al. (2021b). Shared Risk and Protective Factors between Alzheimer's Disease and Ischemic Stroke: A Population-Based Longitudinal Study. *Alzheimers Dement* 17 (2), 191–204. doi:10.1002/alz.12203

Wang, X., Liu, Z., and Shen, L. (2020a). Isoflurane Preconditioning Inhibits Caspase-11-Related Noncanonical Pyroptosis Pathway to Alleviate Hepatic Ischemia-Reperfusion Injury in Mice. *Nan Fang Yi Ke Da Xue Xue Bao* 40 (5), 670–675. doi:10.12122/j.issn.1673-4254.2020.05.09

Wang, Y., Zhang, L., Pan, Y. J., Fu, W., Huang, S. W., Xu, B., et al. (2020b). Investigation of Invigorating Qi and Activating Blood Circulation Prescriptions in Treating Qi Deficiency and Blood Stasis Syndrome of Ischemic Stroke Patients: Study Protocol for a Randomized Controlled Trial. *Front. Pharmacol.* 11, 892. doi:10.3389/fphar.2020.00892

Wilcock, D. M., Vitek, M. P., and Colton, C. A. (2009). Vascular Amyloid Alters Astrocytic Water and Potassium Channels in Mouse Models and Humans with Alzheimer's Disease. *Neuroscience* 159 (3), 1055–1069. doi:10.1016/j.neuroscience.2009.01.023

Xiao, M., Xiao, Z. J., Yang, B., Lan, Z., and Fang, F. (2020). Blood-Brain Barrier: More Contributor to Disruption of Central Nervous System Homeostasis Than Victim in Neurological Disorders. *Front. Neurosci.* 14, 764. doi:10.3389/fnins.2020.00764

Yamazaki, Y., and Kanekiyo, T. (2017). Blood-Brain Barrier Dysfunction and the Pathogenesis of Alzheimer's Disease. *Int. J. Mol. Sci.* 18 (9), 1965. doi:10.3390/ijms18091965

Yi, Y. S. (2018). Regulatory Roles of the Caspase-11 Non-canonical Inflammasome in Inflammatory Diseases. *Immune Netw.* 18 (6), e41. doi:10.4110/in.2018.18.e41

Yu, L., Tao, J., Zhao, Q., Xu, C., and Zhang, Q. (2020). Confirmation of Potential Neuroprotective Effects of Natural Bioactive Compounds from Traditional Medicinal Herbs in Cerebral Ischemia Treatment. *J. Integr. Neurosci.* 19 (2), 373–384. doi:10.31083/j.jin.2020.02.63

Yu, Z., Cai, M., Li, X., Zhang, J., Wu, T., Yang, F., et al. (2018). Neuroprotective Effects of Tongxinluo on Focal Cerebral Ischemia and Reperfusion Injury in Rats Associated with the Activation of the MEK1/2/ERK1/2/p90RSK Signaling Pathway. *Brain Res.* 1685, 9–18. doi:10.1016/j.brainres.2018.01.036

Yu, Z. H., Cai, M., Xiang, J., Zhang, Z. N., Zhang, J. S., Song, X. L., et al. (2016). PI3K/Akt Pathway Contributes to Neuroprotective Effect of Tongxinluo against Focal Cerebral Ischemia and Reperfusion Injury in Rats. *J. Ethnopharmacol* 181, 8–19. doi:10.1016/j.jep.2016.01.028

Zhang, D., Qian, J., Zhang, P., Li, H., Shen, H., Li, X., et al. (2019). Gasdermin D Serves as a Key Executioner of Pyroptosis in Experimental Cerebral Ischemia and Reperfusion Model Both *In Vivo* and *In Vitro*. *J. Neurosci. Res.* 97 (6), 645–660. doi:10.1002/jnr.24385

Zhang, K., Liu, Q., Luo, L., Feng, X., Hu, Q., Fan, X., et al. (2021a). Neuroprotective Effect of Alpha-Asarone on the Rats Model of Cerebral Ischemia-Reperfusion Stroke via Ameliorating Glial Activation and Autophagy. *Neuroscience* 473, 130–141. doi:10.1016/j.neuroscience.2021.08.006

Zhang, S., Jiang, X., Wang, Y., Lin, K., Zhang, Z., Zhang, Z., et al. (2021b). Protective Effect of An-Gong-Niu-Huang Wan Pre-treatment against Experimental Cerebral Ischemia Injury via Regulating GSK-3β/HO-1 Pathway. *Front. Pharmacol.* 12, 640297. doi:10.3389/fphar.2021.640297

Zheng, T., Jiang, H., Jin, R., Zhao, Y., Bai, Y., Xu, H., et al. (2019). Ginsenoside Rg1 Attenuates Protein Aggregation and Inflammatory Response Following Cerebral Ischemia and Reperfusion Injury. *Eur. J. Pharmacol.* 853, 65–73. doi:10.1016/j.ejphar.2019.02.018

Zhou, Y., Li, H. Q., Lu, L., Fu, D. L., Liu, A. J., Li, J. H., et al. (2014). Ginsenoside Rg1 Provides Neuroprotection against Blood Brain Barrier Disruption and Neurological Injury in a Rat Model of Cerebral Ischemia/reperfusion through Downregulation of Aquaporin 4 Expression. *Phytomedicine* 21 (7), 998–1003. doi:10.1016/j.phymed.2013.12.005

Zupanic, E., von Euler, M., Winblad, B., Xu, H., Secnik, J., Kramberger, M. G., et al. (2021). Mortality after Ischemic Stroke in Patients with Alzheimer's Disease Dementia and Other Dementia Disorders. *J. Alzheimers Dis.* 81 (3), 1253–1261. doi:10.3233/JAD-201459

Conflict of Interest: The authors declare that the research was conducted in the absence of any commercial or financial relationships that could be construed as a potential conflict of interest.

Publisher's Note: All claims expressed in this article are solely those of the authors and do not necessarily represent those of their affiliated organizations, or those of the publisher, the editors, and the reviewers. Any product that may be evaluated in this article, or claim that may be made by its manufacturer, is not guaranteed or endorsed by the publisher.

Copyright © 2021 Lyu, Li, Yu, Chan, Fu, Li and Zhang. This is an open-access article distributed under the terms of the Creative Commons Attribution License (CC BY). The use, distribution or reproduction in other forums is permitted, provided the original author(s) and the copyright owner(s) are credited and that the original publication in this journal is cited, in accordance with accepted academic practice. No use, distribution or reproduction is permitted which does not comply with these terms.